Journal of South American Earth Sciences
October 2023, Volume 130, Pages 104503 (16p.)
https://doi.org/10.1016/j.jsames.2023.104503 https://archimer.ifremer.fr/doc/00848/95999/

Structural evolution of the southern Ecuadorian forearc in the Santa Elena Peninsula region

Bulois Cédric [1, *], Saillard Marianne [1], Espurt Nicolas [1], Benítez Pedro Reyes [2], Michaud François [1, 3], Barba Diego [4], Peuzin Andréa [1], Hernández Salazar María José [3], Schenini Laure [1], Régnier Marc [1], Ratzov Gueorgui [1]

[1] Université Côte d'Azur, IRD, CNRS, Observatoire de la Côte d'Azur, Géoazur, Valbonne, France
[2] Departamento de Geología, Facultad de Ingeniería en Geología y Petróleos, Escuela Politécnica Nacional, Ladrón de Guevara E11-253, PO. Box, 17-01-2759, Quito, Ecuador
[3] Sorbonne Université, Faculté des Sciences et Ingénierie, F-75252, Paris, France
[4] Petroamazonas EP, Av. 6 de Diciembre y Gaspar Cañero, Quito, Ecuador

* Corresponding author : Cédric Bulois, email address : bulois@geologie.ens.fr

Abstract :

The southern Ecuadorian forearc system is related to the subduction of the oceanic Farallon/Nazca Plate beneath the continental South American Plate since the Late Cretaceous, and currently evolves with the dynamic of a tectonic block called North Andean Sliver. To explore the structural architecture and processes controlling the Upper Cretaceous-Cenozoic growth of the forearc, we built a ~143 km-long onshore-offshore crustal-scale cross-section in the Santa Elena Peninsula region using seismic reflection profiles and well and field data. The structure of the Santa Elena Peninsula forearc system is controlled by imbrication of Upper Cretaceous-Palaeocene oceanic basement and Cenozoic sedimentary units, and underplating of distal Cenozoic sequences stacked at the trench zone. This led to the progressive construction of an accretionary wedge through time. The forearc substratum is mainly formed by the Upper Cretaceous-Palaeocene basement developed during the docking of oceanic terranes. It is later deformed by NW-trending landward-dipping, normal to strike-slip faults during the Middle Eocene, and renewed compression by inversion of inherited faults from the Oligocene onwards. Recent deformation consists in N-trending oceanward-dipping normal faults in the frontal slope domain and fault-controlled uplift of marine terraces along the coastal area. Therefore, the Upper Cretaceous to present-day structural evolution of the Santa Elena Peninsula forearc is controlled by the long-lasting subduction dynamics and structural inheritance of the upper plate.

Highlights

► We illustrate the structural architecture of the Santa Elena Peninsula forearc system. ► It is dominated by compression punctuated by zones/episodes of normal to strike-slip faulting. ► Its evolution reflects the subduction dynamics and the upper plate structural inheritance.

Keywords : forearc, structural inheritance, Northern Andes, Ecuador

1. Introduction

The structural framework of a forearc result from the vertical stack of structural units formed by basement rocks, marine sediments and volcanics scrapped off the subducting oceanic plate (Dickinson and Seely, 1979; Moore *et al.*, 2001; Stern, 2002; Cawood *et al.*, 2009; Noda, 2016). Depending on time duration and the geometric evolution of the subduction zone, a forearc system may involve one or several fold-thrust belts and depocentres younging oceanward, emplaced ahead of the inner crustal wedge (orogenic wedge/magmatic arc;

François *et al.*, 2021). The velocity and direction of the convergence, slab dip and amount of sediments at the trench significantly influence the accretion or erosion style of the forearc (Dahlen, 1990; von Huene and Scholl, 1991; Le Pichon *et al.*, 1993; Lallemand *et al.*, 1994; Collot *et al.*, 2002; Gutscher and Westbrook, 2009; Noda, 2016). Normal faulting often occurs as a result of gravitational forces expressing a localised and progressive collapse in parallel to the margin uplift (Vannucchi *et al.*, 2008 and 2012; Wang *et al.*, 2010). Extension is produced by erosive degradation of the margin (Armijo and Thiele, 1990; Bourgois *et al.*, 1993; von Huene *et al.*, 1999; Clift and Vannucchi, 2004; Sallarès and Ranero, 2005), frontal erosion due to seamounts subduction (Dominguez *et al.*, 1998; Vannucchi *et al.*, 2004), or interseismic loading and coseismic/postseismic strain release during earthquakes (Delouis *et al.*, 1998; Loveless *et al.*, 2005). Therefore, gravitational forces constantly reshape the forearc morphology to keep slope stability, especially in sedimentary-overfilling environments where non-cohesive material likely deposits (Hamblin and Christensen, 1995). This implies a combination of crustal and surficial processes (*i.e.* subduction-erosion, structural equilibrium, sedimentary growth) switching between short and long-term phases, inherent to the progressive construction of a long-lived forearc system likely recording the subduction evolution (Espurt *et al.*, 2018).

This study focusses on the Santa Elena Peninsula region located along the South Ecuadorian forearc zone (Fig. 1). This segment of the margin is marked by a relatively moderate seismicity mixing thrust, strike-slip and normal focal mechanisms (Beauval *et al.*, 2010, 2013; Font *et al.*, 2013; Yepez *et al.*, 2016; Vaca *et al.*, 2019), and is usually described as erosional (Lonsdale, 1978; Sage *et al.*, 2006; Hernández *et al.*, 2020). The development of normal faults cutting through the upper plate down to the subduction interface are classically interpreted as a result of basal erosion due to subducting asperities and/or of the oblique convergence (Collot *et al.*, 2002, 2008a, 2008b and 2011; Calahorrano Bétancourt, 2005; Sage *et al.*, 2006; Bourgois *et al.*, 2007; Ratzov *et al.*, 2012). Regional tectonostratigraphy suggests an overall accretion framework, associated with synchronous normal faulting since the Late Cretaceous across southern Ecuador and northern Peru (Daly, 1989; Benítez, 1995; Espurt *et al.*, 2018; Aizprua *et al.*, 2019; Hernández *et al.*, 2020; Jaillard, 2022).

This paper aims to identify structural mechanisms that controlled the large-scale evolution of the Santa Elena Peninsula forearc over the Late Cretaceous-Cenozoic period by highlighting the onshore-offshore links between shallow and deep structures. Despite many geological integrations of surface and subsurface data (*e.g.* Benítez, 1995; Reyes, 2013; Aizprua *et al.*, 2019; Witt *et al.*, 2019; Hernández *et al.*, 2020; Jaillard, 2022), the onshore-offshore continuity of tectonic structures and their geometry remain uncertain. This approach is essential to correlate the morphotectonic expression of the margin with seismic hazards as functions of successive short- and long-term processes.

2. Structural framework of the Santa Elena Peninsula region

The southern Ecuador deformation is dominated by the subduction of the Farallon/Nazca plates beneath South America controlling the northeastward tectonic escape of the North Andean Sliver along the Puná-Pallatanga Fault, a crustal-scale, segmented, dextral strike-slip fault belonging to the Dolorès-Guayaquil Fault Zone running from the Gulf of Guayaquil in Ecuador to Venezuela (Fig. 1; Pennington, 1981; Freymueller *et al.*, 1993; Kellog and Vega, 1995; Trenkamp *et al.*, 2002; White *et al.*, 2003; Nocquet *et al.*, 2014; Villegas-Lanza *et al.*, 2016). Located at the southwesternmost part of the North Andean Sliver, the Santa Elena Peninsula region belongs to an onshore-offshore Upper Cretaceous-to-Quaternary forearc system containing the Valdivia Basin to the north, the Guayaquil Basin to the south, and the Progreso Basin to the east, all three surrounded by a system of cordilleras (Fig. 1b). Between ~75 and 55 Ma, the convergence controlled the amalgamation of ocean-derived terranes, outcropping nowadays in the Coastal and Chongón-Colonche cordilleras and locally in the Santa Elena Peninsula region (Hey, 1977; Feininger and Bristow 1980; Reynaud *et al.*, 1999; Audemard and Audemard, 2002; Kerr *et al.*, 2002; Jaillard *et al.*, 2004, 2008 and 2009; Lonsdale, 2005; van Melle *et al.*, 2008; Vallejo *et al.*, 2009; Reyes and Michaud, 2012; Jaillard, 2022). Compression continued during the Eocene, Oligocene and Miocene with the development of fold-and-thrust belts and forearc depocentres (Benítez, 1995; Jaillard *et al.*, 1995, 1997; Aizprua *et al.*, 2019; Witt *et al.*, 2019; Hernández *et al.*, 2020; Alemán *et al.*, 2021). Altogether, this led to significant clockwise rotation of the Ecuadorian forearc and localised dextral strike-slip motions along inherited faults (Pennington, 1981; Roperch *et al.*, 1987; Jaillard *et al.*, 2009; Egbue and Kellogg, 2010; Amórtegui *et al.*, 2011; Alvarado *et al.*, 2016; Baize *et al.*, 2020; Siravo *et al.*, 2021).

The modern structural evolution of the Santa Elena Peninsula region is likely controlled by the roughness of the lower plate but debates exist on the timing and magnitude of regional tectonic events. In particular, the subduction of the Carnegie Ridge under the southern Ecuadorian forearc (Fig. 1) started either ~8-15 Ma ago (Daly, 1989; Gutscher *et al.*, 1999; Schütte *et al.*, 2010), ~3-5 Ma ago (Collot *et al.*, 2008a and 2009; Michaud *et al.*, 2009 and 2018) or ~1-2 Ma ago (Lonsdale and Klitgord, 1978). The ridge corresponds to a ~200 km-wide, 2 km-high, 80°N-trending bathymetric high, composed of 14 to 19 km-thick oceanic crust originated from the Galapagos Hotspot (Sallarès and Charvis, 2003; Graindorge *et al.*, 2004; Harpp *et al.*, 2004). Its subduction likely triggered seaward-dipping normal faulting favouring overpressured fluids migration in the subduction channel (Calahorrano Bétancourt, 2005; Sage *et al.*, 2006; Proust *et al.*, 2016), coastal uplift up to 200-to-300 m high witnessed by Upper Pliocene-to-Lower Pleistocene marine terraces (Cantalamessa and Di Celma, 2004; Pedoja *et al.*, 2006a and 2006b), as well as exhumation of crustal rocks and variations of drainage patterns in the Coastal Cordillera (Daly, 1989; Benítez, 1995; Aalto and Miller, 1999; Deniaud *et al.*, 1999; Witt *et al.*, 2006; Reyes, 2013; Collot *et al.*, 2019; Hernández *et al.*, 2020; Brichau *et al.*, 2021). Finally, the development of the Puná-Pallatanga Fault (Fig. 1b) could also be associated to the subduction of the ridge (Deniaud *et al.*, 1999; Deniaud, 2000; Witt *et al.*, 2006, Bourgois *et al.*, 2007; Cobos and Montenegro, 2010; Witt and Bourgois, 2010).

3. Stratigraphy of the onshore domain

The following description provides a synthesis of the onshore stratigraphy of the Santa Elena Peninsula region based on an extended literature review (Fig. 2). This is required to support our investigation offshore (Section 4), in order to highlight the extent of regional episodes and their influence throughout the margin.

3.1. Upper Cretaceous-Palaeocene basement

To the northeast, the Santa Elena Peninsula region is bounded by the Chongón-Colonche Cordillera (Fig. 1b), a massif composed of Upper Cretaceous arc-derived volcanoclastics and crystalline rocks of oceanic origin (Goossens and Rose 1973; Jaillard *et al.* 1995 and 2009; Reynaud *et al.*, 1999; Mamberti, 2001; Luzieux *et al.*, 2006; van Melle *et al.*, 2008; Seyler *et al.*, 2021; Jaillard, 2022). The basement also outcrops irregularly across the coastal zone (Benítez, 1995; Luzieux *et al.*, 2006; Reyes and Michaud, 2012) and extends offshore (Aizprua *et al.*, 2019; Hernández *et al.*, 2020). It is composed of highly-deformed Coniacian tholeiitic basalts and pillow-lavas (*Piñon Fm*) covered by dacitic breccias (*Las Orquideas Fm*), Middle Coniacian-Lower Campanian siliceous limestones and radiolarian mudstones (*Calentura Fm*), and Upper Campanian-Maastrichtian flysch and volcanoclastics (*Cayo Fm*) (Fig. 2). These formations are overlain by an Upper Maastrichtian-Upper Palaeocene clastic wedge, composed of distal sandstones, siltstones and cherts (*Guayaquil Fm*) and highly-deformed tuffaceous and pelagic black cherts (*Santa Elena Fm*). Depending of the region of observation, the *Guayaquil Fm* is either quartz-free and therefore pre-accretionary in age (Jaillard *et al.*, 2009) or postaccretionary due to volcanic zircon grains originated from a continental volcanic arc in the Western Cordillera (Vallejo *et al.*, 2009, 2019). Similarly, the *Santa Elena Fm* is alternatively interpreted as an olistostrome (Azad, 1964; Colman, 1970; Bristow and Hoffstetter, 1977) or as pre-accretionary deposits (Jaillard *et al.*, 1995, 2009; Aizprua *et al.*, 2019). These formations are unconformably covered by uppermost Palaeocene coarse-grained quartz-rich turbidites (*Azúcar Fm*) sourced from the continent (Jaillard *et al.*, 1995; Witt *et al.*, 2019; Jaillard, 2022). In this study, the Upper Cretaceous-Palaeocene rocks form a basement developed during the progressive establishment of ocean-derived terranes accreted to the margin and shedding sediments following the erosion of uplifted terranes. This period of oceanic terrane docking took place from the Late Campanian until the Late Palaeocene.

3.2. Eocene unit

The regional unconformity U1 (Fig. 2) marks the contact between the Upper Cretaceous-Palaeocene basement and the Middle Eocene succession (Jaillard, 2022). These are known as the *Ancón Group*, which is composed of basal shales deposited in an unstable marine environment (*Clay Pebble Beds Fm*), middle turbidites, siltstones and claystones composing submarine fans (*Socorro Fm*), and upper siltstones and sandstones witnessing outer-shelf conditions (*Secca Fm*). The *Ancón Group* is overlain by a Middle Eocene transgressive-regressive sequence (*San Mateo Fm*) in the Chongón-Colonche Cordillera and unconformable, coarse-grained sandstones, possibly turbiditic in places, alternating with thin shales (*Punta Ancón Fm*; Bristow and Hoffstetter, 1977; Jiménez and Mostajo, 1989; Benítez, 1995; Jaillard *et al.*, 1995; Luzieux, 2007; Jaillard, 2022).

3.3. Oligocene unit

The Eocene-Oligocene transition is characterised by the regional unconformity U2 (Fig. 2), contemporaneous with the breakup of the Farallon Plate (Benítez, 1995; Jaillard *et al.*, 1995;

Ordoñez *et al.*, 2006; Jaillard, 2022). Oligocene strata correspond to shallow marine transgressive conglomerates and sandstones (*Zapotal Fm;* Benítez *et al.*, 1986).

3.4. Neogene unit

Overlying Miocene sequences accumulated mainly in the Progreso Basin (Fig. 2) in local depocenters developing along the cordilleras (Bristow and Hoffstetter, 1977; Deniaud, 2000; Reyes and Michaud, 2012; Reyes, 2013; Eguëz *et al.*, 2019). Strata consist in Aquitanian-Lower Burdigalian marine sandstones, siltstones and shales (*Dos Bocas Fm*), Upper Burdigalian diatomaceous siltstones and mudstones (*Villingota Fm*), Langhian-Lower Serravallian calcareous siltstones and sandstones (*Subibaja Fm*), Upper Serravalian to Messinian channelised fine sands intercalated with siltstones and shales (*Progreso Fm*), uppermost Messinian to Pliocene sandstones (*Puna Fm*), and conglomerates, sandstones and siltstones (*Balzar Fm*).

3.5. Quaternary unit

Clastic deposition continued during the Pleistocene (*Tablazo Fm*) in parallel with the development of marine terraces along the coast (Pedoja *et al.*, 2006a; Reyes, 2013). Unconformable Holocene strata are characterised by non-consolidated sediments (*Llanura Fm*) associated with river systems or alluvial and marine terraces (Pedoja *et al.*, 2006a; Reyes, 2013; Eguëz *et al.*, 2019). The two formations are unconformably deposited on previous sediments (unconformity U3) and are contemporaneous with extensional tectonics in the Guayaquil Basin (Fig. 2; Deniaud, 2000; Witt *et al.*, 2006; Cobos and Montenegro, 2010).

4. Onshore-offshore stratigraphic correlation

The stratigraphic description in Section 3 highlights the sedimentary succession outcropping in the onshore Santa Elena Peninsula region, and stratigraphic correlation with the offshore domain is challenging due to sparse drilling information in the offshore domain (Figs

3 and 4). Based on gamma ray and sonic logs analysis (Serra, 1979 and 1995), we propose a description of offshore sedimentary sequences of Well B1-NSX1-1X drilled in the Valdivia Basin (provided by Petroamazonas EP, initially drilled by Belco Petroleum Ecuador Inc in 1988). The stratigraphic content is partially reinterpreted compare to well reports as it takes into account age reappraisal (Ordoñez *et al.*, 2006) and the most recent geological descriptions along the coastal area (Reyes and Michaud, 2012; Reyes, 2013; Aizprua *et al.*, 2019; Witt *et al.*, 2019; Jaillard, 2022). We also use Well B1-MT1-1X (Montañita-1; Aizprua *et al.*, 2019; Hernández *et al.*, 2020) located on the northern edge of the Valdivia Basin to extend our observations to the northwest. The main lithostratigraphic surfaces are then seismically controlled (Fig. 5).

Well B1-NSX1-1X bottomed ~70m-thick, siltstones and claystones deposited in a shallow-to-deep marine environment (Fig. 4), that are similar to onshore Upper Cretaceous clastics of the *Cayo Fm* (Benítez, 1995; Jaillard *et al.*, 1995 and 2009; Luzieux *et al.*, 2006). This implies that underlying sediments, belonging to the *Piñon* and *Calentura Fms*, likely extend below drilling sites. Thin poorly-dated, 50m-thick Palaeocene-Lower Eocene shallow marine siltstones are recovered in Well B1-NSX1-1X, which are described as a condensed sequence equivalent to the *Santa Elena* or the *Azúcar Fms* in well reports (Benítez, 1995; Jaillard *et al.*, 1995; Keller *et al.*, 1997; Luzieux, 2007; Aizprua *et al.*, 2019). Thus, we correlate the onshore Upper Cretaceous-Palaeocene basement westward. It is topped by the Middle Eocene unconformity U1 of varying magnitude across the Santa Elena Peninsula region.

In Well B1-NSX1-1X, 1630m-thick Middle Eocene strata correspond to shallow-marine siltstones and mudstones and occasional carbonates (Fig. 4). Similar strata (1830m-thick) are reported in Well B1-MTX1-1X, with notable tuff levels similar to the ones radiometrically dated at 53.7±1.4 Ma (*i.e.* Ypresian; Witt *et al.*, 2019), which remains uncorrelated to any known sedimentary intervals offshore. Well reports attributed a much thicker interval (~2280m) to the *Ancón Group* despite an insufficient biostratigraphic content to determine a more accurate age. Here, we consider that these Middle Eocene strata are thinner than previously proposed in well reports, but are thicker than those measured onshore (~1000m-thick; Reyes, 2013).

Overlying strata consist in poorly-dated Upper Eocene sandy deposits intercalated with muds and siltstones in Well B1-NSX1-1X (Fig. 4), and extend into similar facies in Well B1-MTX1-1X. Well reports and Jaillard *et al.* (1995) originally interpreted these as the uppermost *Ancón Group* (turbidites of the *Socorro Fm.* and shoreface deposits of the *Pta Ancon Fm.*), which are consistent with a global regression, but these boundaries remain difficult to correlate with seismic data through the region. We rather correlate this sequence with conglomerates and occasional mudstones and siltstones of the *Zapotal Fm*. Therefore, a Late Eocene age is unlikely so that we regard this interval as a deeper equivalent of onshore Oligocene unit that may extend into the lowermost Miocene (Benítez, 1995; Deniaud, 2000; Luzieux, 2006; Ordoñez *et al.*, 2006; Reyes, 2013). This is consistent with the presence of Oligocene-Miocene sandstones radiometrically dated at 29.5±0.4 and 23.5±0.6 Ma north of the Valdivia Basin (Witt *et al.*, 2019), in continuation of the Progreso Basin (Alemán *et al.*, 2021).

In Well B1-NSX1-1X, we interpret an ~100m-thick Neogene unit, comparable to the ~400m-thick uppermost sediments of the Progreso Basin (Bristow and Hoffstetter, 1977; Benítez, 1995; Deniaud, 2000; Eguëz *et al.*, 2019) and to the ~3000m-thick strata along the southwestern littoral zone (Reyes, 2013). This suggests that a major part of the Neogene unit has been eroded or non-deposited in the Valdivia Basin (Hernández *et al.*, 2020). It is unconformably covered by ~250m-thick Quaternary sediments (unconformity U3) made of sandstones and siltstones equivalent to the *Tablazo Fm* and conglomerates to the *Llanura Fm*. Even though this sedimentary interval was originally thought to belong exclusively to the *Ancón Group* in well reports, we argue here that the uppermost strata are younger and likely present significant thickness variations.

5. Surface and subsurface data

The Santa Elena Peninsula, Valdivia Basin and Progreso Basin zones provide a good exposure of geological structures (Benítez, 1995; Jaillard *et al.*, 1995; Reyes and Michaud, 2012; Aizprua *et al.*, 2022). These are dated with sedimentary units as described in the above (Section 3) using basic seismic correlation (Mitchum *et al.*, 1977; Vail *et al.*, 1977; Badley, 1985). Numerous two-dimensional hydrocarbon seismic reflection profiles provide a good imaging of the platform (1-to-2km-spaced seismic lines shot in 1986 across the platform by *Belco Petroleum* and *Western Geophysical*, reprocessed by PetroEcuador). They are supplemented by ~5 km-spaced seismic profiles acquired perpendicularly to the trench by *SCAN Geophysical ASA* (processed by SINOPEC) and academic profiles of SISTEUR and ATACAMES surveys (IFREMER and Instituto Oceanográfico de la Armada del Ecuador).

5.1. Structural mapping

Field, well and seismic profile data are combined with long-wavelength gravity data and high-resolution aero-gravity data (Hernández *et al.*, 2020) to construct a structural map of the Valdivia Basin-Santa Elena Peninsula region and northern edge of the Progreso Basin (Fig. 3). Map analysis is systematically compared to published detailed onshore and offshore studies (Reyes and Michaud, 2012; Aizprua *et al.*, 2019 and 2022; Hernández *et al.*, 2020).

Our structural map (Fig. 3) shows that the forearc is composed of six structural domains in the Santa Elena Peninsula region. Landward to seaward, these units are the Chongón-Colonche Cordillera (+90 to +100 mgal), the triangular-shaped Progreso Basin (+20 to -110 mgal), the ~N-trending Santa Elena High-Valdivia Basin-Monteverde Basin domain (+40 to +60 mgal), the ~N-trending slope basin (+20 to -60 mgal), the ~N-trending trench basin (-60 mgal) and the subducting oceanic Nazca Plate (0 to +30 mgal). Faults are grouped according to their orientation. The onshore domain and the platform domain between the Santa Elena Peninsula and the La Plata Island are characterised by N130°E-trending northeast-dipping normal fault systems notably parallel to the Chongón-Colonche Cordillera and Carrizal normal fault system of mostly Late Cretaceous-Palaeocene age (Fig. 3). The Progreso depocenter is bounded southwestward by the N140°-160°E La Cruz Fault system formed of the Oligocene and Neogene. Our interpretation also confirms the presence of NW-SE normal faults in the offshore domain delimiting the Valdivia and Monteverde depocentres as proposed by Hernández *et al.* (2020). Therefore, all these structures imply a deep structural control, suggesting that the margin belongs to a wide compressional zone extending across the Santa Elena Peninsula region, the Progreso Basin and the Guayaquil Basin as recently proposed by Witt *et al.* (2019) and Aizprua *et al.* (2022). Finally, the slope domain is characterised by N-to-N10°E-trending, oceanward-dipping normal faults notably parallel to the trench, implying that they formed, at least to a certain extent, in relation with subduction processes (Sage *et al.*, 2006).

5.2 Cross-sectional structural architecture and kinematics

The structural architecture of the Santa Elena Peninsula forearc is shown on Figure 5 through an ~143km-long synthetic cross-section (B90-46, part of B90-50, part of E86-183B and MR08-756) linking the northern edge of the Progreso Basin to the trench (Fig. 3). Reflectors of the upper plate are calibrated using surface data in the onshore domain (Daly, 1989; Reyes and Michaud, 2012) and offshore Well B1-NSX1-1X (Fig. 4). Our interpretation highlights the main characteristics of structural domains mentioned in Subsection 5.1.

The Chongón-Colonche Cordillera corresponds to a major homocline made of Upper Cretaceous-Palaeocene basement unconformably covered by Neogene strata (Fig. 1). Its structural interpretation is only constrained by field data. Reyes and Michaud (2012) proposed that the cordillera is separated from the Progreso Basin and the Santa Elena Peninsula by steep southwest-dipping normal faults. Instead, Daly (1989) suggested that it overthrusted the Progreso Basin southwestward during the Neogene. In contrast, we propose here that the

Chongón-Colonche Cordillera corresponds to a palaeo-horst system later transported onto a southwest-verging blind thrust.

The structural interpretation of onshore seismic profiles B90-46 and B90-50 (Annexe 1) together with surface data show that the Progreso Basin corresponds to an asymmetric syncline of Eocene-to-Miocene strata (Fig. 5). The basin depth (base of the Eocene unit), approximately constrained at ~2 sTWT (~2.5 km), is consistent with the northwestward elevation of the basin bottom (Aizprua *et al.*, 2022). The Progreso Basin is bounded by the Carrizal fault system to the northeast and the La Cruz fault system to the southwest (Fig. 3). The two faults may correspond to reactivated deep-seated faults inherited from a Middle-Late Eocene period of extension, as already proposed by Hernández *et al.* (2020), and consistent with the Middle-Late Eocene deep marine environment of the *Ancón Group* (Fig. 4). During the Oligocene and Early Miocene (roughly *Zapotal Fm*), the two faults were reactivated by inversion tectonics, resulting in the formation of the basin as it is today. In addition to thrusting, Aizprua *et al.* (2022) also suggested additional strike-slip deformation, which is not dismissed in our analysis. However, our interpretation of the Oligo-Miocene period in the Progreso Basin differs substantially from continuous transtensional opening proposed by Alemán *et al.* (2021). Thus, we interpret the Carrizal fault system at depth as a west-verging thrust affecting the Upper Cretaceous-Palaeocene basement, intermittently reactivated (positively or negatively) during the Eocene and the Oligo-Miocene (Fig. 5). In comparison, the La Cruz fault system corresponds to thrusts propagating westward with shortcut trajectories through northeast-dipping normal faults.

West of the Progreso Basin, Middle Eocene rocks lie unconformably on Upper Cretaceous-Palaeocene basement outcropping immediately to the north (Fig. 5). This zone, called Santa Elena anticline, corresponds to an ~17km-wide sub-continuous coastal bulge extending across the Santa Elena Peninsula region and made of tilted Middle-to-Upper Eocene strata controlled at depth by imbricate structures in the Upper Cretaceous-Palaeocene basement related to the La Cruz fault system.

Correlation of seismic profiles E86-183B and MR08-756 with Well B1-NSXI-IX (Annexes 1 and 2) shows an Upper Cretaceous-Palaeocene basement that extends across the offshore part of the Santa Elena Peninsula region to the trench zone (Fig. 5). This interpretation is consistent with outcrops in the La Plata Island and seismic analysis in the Valdivia Basin region (*e.g.* Michaud *et al.*, 2012; Egüez *et al.*, 2019; Hernández *et al.*, 2020). The basement of the Valdivia Basin is covered by ~2.2 km-thick Eocene-to-Quaternary sedimentary units. West of Well B1-NSXI-IX, these units are deformed by major landward-dipping thrust faults and an outer pop-up structure testifying of the overall uplift of the margin. The shortening is most likely contemporaneous with the deposition of Oligocene-Miocene sedimentary units in the onshore domain. We argue that faults in the Valdivia Basin mark the continuation of the Carrizal and La Cruz fault systems (Progreso Basin) and show a similar reactivation evolution.

Quaternary marine terraces witness that the coastal zone, including the Santa Elena anticline, has been recently uplifted (Pedoja *et al.*, 2006a; Cisneros Medina, 2018). At the westernmost point of the Santa Elena Peninsula, the Punta Salinas (so-called the La Chocolatera) exhibits 4 levels of staircase marine terraces between ~2 m and >80 m above sea level (Fig. 6; Pedoja *et al.*, 2006a). The projection of the Punta Salinas onto seismic lines (~11 km north) shows a continuation of the uplift through outer pop-up structures (Figs 3 and 5).

Finally, the western part of the seismic profile MR08-756 (see Annexe 2) shows that the slope domain is characterised by major oceanward-dipping listric extensional faults (Fig. 5). These faults reach at depth the Upper Cretaceous-Palaeocene basement, coinciding locally with possible bottom simulating reflectors (BSR) and controlling notable thickness variations in Eocene and Neogene sequences. At the trench, the development of a small frontal accretionary prism involves Neogene-Quaternary units (Sage *et al.*, 2006), that we interpret beneath the overriding Upper Cretaceous-Palaeocene basement. Its morphology is also likely controlled by the rough topography of the subducting oceanic Nazca Plate, including major asperities (high-dipping normal faults and seamounts) and thin oceanic sediments thickening toward the trench (Fig. 5).

6. Structural evolution of the Santa Elena Peninsula region

The above structural interpretation shows that the Santa Elena Peninsula region recorded intermittent compressional and extensional deformation since the Late Cretaceous. This formed a complex forearc controlled by crustal-scale thrusts and normal faults (Figs. 3 and 5). We specifically discuss the various mechanisms responsible for the formation and kinematics of faults compare to the dynamics of the Farallon/Nazca Plate subduction and speculate on fault reactivation processes in the overriding plate over time.

6.1. Late Cretaceous to Early-to-Middle Eocene

The amalgamation of oceanic terranes beneath the North Andean continental margin of Ecuador took place from the Late Maastrichtian to the Late Palaeocene (Reynaud *et al.*, 1999; Spikings *et al.*, 2001; Jaillard *et al.*, 2004, 2008 and 2009; Aizprua *et al.*, 2019; Vallejo *et al.*, 2019; Jaillard, 2022). The oceanic terrane accretion occurred in a ~N60°E-directed convergence at a rate of ~60 mm.yr^{-1} (Fig. 7; Pardo-Casas and Molnar, 1987; Somoza and Ghidella, 2012). The resulting fold-thrust belt and the related uplift of the upper plate are coeval of unconformities and syn-tectonic sediments sourced from the basement (*e.g. Azucar Fm*). The oceanic terrane docking evolution is sealed by the Middle Eocene unconformity U1 (Fig. 4), which is consistent with a regional hiatus during the Early-to-Middle Eocene (Jaillard *et al.*, 1997; Jaillard, 2022).

The northern Andean forearc has accommodated major clockwise rotation rating from 60-70° during the Cretaceous to 20-30° after the Late Miocene (Roperch *et al.*, 1987; Luzieux *et al.*, 2006; Siravo *et al.*, 2021). This implies a modification of initial structural trends through time. We speculate that numerous east-dipping normal and reverse faults in the modern forearc correspond to former thrusts or strike-slip faults formed during the oceanic terrane docking event. Thus, the structure of the Chongón-Colonche Cordillera is probably inherited from this period, with Late Cretaceous thrust faults formed along a presumably NW-SE to WNW-ESE direction due to the roughly 60°-directed convergence between the Farrallon and the South America plates (Fig. 7; Pardo-Casa and Molnar, 1987). During the Early Eocene onwards, accreted terranes recorded at least 20°-clockwise progressive rotation due to the ongoing compression, that expressed variably across the region depending on the direction of former thrusts (Luzieux *et al.*, 2006). From our point-of-view, this explains part of the curved morphology of the present-day Chongón-Colonche Cordillera, as well as former thrusts in the Monteverde, Valdivia and Progresso basins before their reactivation from the Middle-to-Late Eocene (Figs. 3 and 5). Therefore, we consider a large accretionary system growing progressively westward from the Late Cretaceous to the end of the Early Eocene, which is consistent with previous regional studies (Jaillard *et al.*, 1997; Jaillard, 2022).

6.2. Middle-to-Late Eocene

During the Middle and Late Eocene, the Progreso, Santa Elena Peninsula and Valdivia areas encompassed a generalised transgression and subsidence. These were synchronous to small-scale normal faulting in the Progreso Basin (Jaillard *et al.*, 1997) and, at a wider extent, to volcanogenic massive sulfide deposits, attributed to the extension of the Macuchi block (central Ecuador) dated between 41.49±0.37 Ma and 42.13±0.54 Ma (Vallejo *et al.*, 2016). Altogether, this undersigns large-scale extension across the forearc. In the Santa Elena Peninsula region, these movements are consistent with the reactivation of Upper Cretaceous-to-Eocene basement thrusts as normal faults during the Middle Eocene (Fig. 5). Middle Eocene extension is sealed by the Upper Eocene-Oligocene unconformity U2.

Similar normal faulting and subsidence are recorded in the Middle Eocene of the Talara depocentre in Peru, suggesting extension through most of the North Andean forearc system (*e.g.* Séranne, 1987; Fildani *et al.*, 2008; Espurt *et al.*, 2018). However, extensional forces are poorly constrained regionally. At the time, the subduction of the Farallon Plate beneath the South American Plate remains ~N70°E-directed but is coeval to a higher convergence rate of 95 mm.yr^{-1} compared to the Late Cretaceous-Palaeocene period (Fig. 7; Somoza and Ghidella, 2012). Therefore, crustal normal faulting in the upper plate could result from transtension controlled by the obliquity of the subduction. It may also be driven by basal erosion at the slab interface related to the subducting plate morphology and/or the increase of convergence rate, as observed in other subduction zones (von Huene and Lallemand, 1990; Le Pichon *et al.*, 1993; Lallemand *et al.*, 1994; von Huene *et al.*, 2004; Sage *et al.*, 2006). Finally, a combined effect of both the subduction obliquity and variations in convergence rates is also possible.

6.3. Latest Eocene-Oligocene to Neogene

The latest Eocene-Oligocene period begins with a regional unconformity produced by the erosion of the former platform, followed by contractional deformation and limited sedimentation across the forearc system, except in the Progreso and Valdivia basins due to fault reactivation and subsidence (Fig. 5). This coincides with a major motion change of the Farallon Plate before its rifting into the Cocos and Nazca plates at ~24 Ma (Fig. 7; Hey, 1977; Lonsdale, 1978; Lonsdale and Klitgord, 1978; Tebbens and Cande, 1997; Lonsdale, 2005; Barckhausen *et al.*, 2008; Seton *et al.*, 2012). To a certain extent, this implies variations in subduction processes due to the presence of a younger, hotter and low-density oceanic plate. Resulting plate reorganisation is synchronous with an acceleration of the convergence rate from 95 mm.yr^{-1} to ~145mm.yr^{-1} at an angle of ~N80°E (Fig. 7; Pardo-Casas and Molnar, 1987; Somoza and Ghidella, 2012). The whole margin likely recorded such an acceleration, leading to fault reactivation and uplift of the margin. A similar uplift is recognised from North Peru to North Ecuador (Espurt *et al.*, 2018; Hernández *et al.*, 2020).

Contractional deformation and uplift of the margin continued at the Miocene-Pliocene transition (Fig. 5). This period is concomitant with the progressive deceleration of the Nazca-South America convergence from 140 mm.yr^{-1} to ~80 mm.yr^{-1}, while the convergence azimuth remained ~N80°E-directed (Fig. 7; Pardo-Casas and Molnar, 1987, Daly, 1989; Norabuena *et al.*, 1999). Such a deceleration could be explained by an increasing load of the continental plate due to the Andes growth, the appearance of flat slab segments beneath South America or thermomechanical variations of the Nazca Plate when penetrating into the transition zone and lower mantle (Yáñez and Cembrano, 2004; Martinod *et al.*, 2010; Quinteros and Sobolev, 2013).

6.4. Quaternary

Quaternary tectonics in Ecuador is associated to the subduction of the Carnegie Ridge and the northeastward tectonic escape of the North Andean Sliver along the Puná-Pallatanga Fault (Fig. 1; Lonsdale, 1978; Lonsdale and Klitgord, 1978; Pilger, 1984; Daly, 1989; Gutscher *et al.*, 1999; Steinmann *et al.*, 1999; Cantalamessa and Di Celma, 2004; Witt *et al.*, 2006; Bourgeois *et al.*, 2007; Alvarado *et al.*, 2016; Baize *et al.*, 2020). We propose that the unconformity U3 marking the Neogene-Quaternary transition (Pleistocene; Fig. 2) is related to this tectonic event. Quaternary compression and extension led to complex faulting and notable thickness variations across the Santa Elena Peninsula region, such as thin Pleistocene strata in the Valdivia Basin affected by reactivated thrusts that thicken in the slope domain due to normal faults (Fig. 5). This leads to the formation of specific morphological features like the modern frontal wedge at the trench, pop-ups on the platform and uplifted marine terraces along the coastal zone.

Quaternary thrusting along the platform domain appears very minor compared to any previously-described deformation phases (Fig. 5). Although this may be regarded as an observation bias due to the relatively-modern formation of pop-ups and marine terraces, this could alternatively reflect that the overall margin is homogeneously uplifting and only minor fault displacements express local tectonic readjustments. In this case, the modern platform domain may express the settlement of a single, relatively rigid block that would correspond to an oceanward-widening backstop system comparable to the pre-Miocene setting centred on the Chongón-Colonche Cordillera. This may mark the onset of the modern North Andean Sliver tectonics, and namely strike-slip motion along the Puná-Pallatanga Fault (Fig. 1).

In the frontal part of the margin, we observe numerous recent normal faults (Fig. 5) that are classically interpreted by subduction-erosion processes (Collot *et al.*, 2002; Sage *et al.*, 2006). However, these structures show a peculiar 5-to-50km-long extensional length, which appears much longer than fault systems developing in similar contexts (*e.g.* 10-15km mega-lenses off Costa Rica and Nicaragua described by Ranero and von Huene (2000), 1-30km offshore crustal normal faults of the Southwest Hellenic Forearc described by Veliz-Borel *et al.* (2022) or <30km-long, possibly discontinuous crustal normal faults along the Alaska to Aleutian Subduction Zone by Kahrizi *et al.* (2023)). We also observe that these normal faults coincide with shallow (~500 m deep) BSR through the trench-slope domain (Fig. 5). Overpressured fluids likely lubricate the subduction interface beneath the continental slope and, added to the general Quaternary uplift of the margin, facilitate the formation of upper gravitational instabilities driven by shallow normal faults in the slope domain. Therefore, this implies that subduction-erosion processes are only locally encountered at the trench-slope domain at Present.

Pop-up structures observed along the western boundary of the Valdivia Basin at a depth of ~120 m below sea level are in agreement with a continuous regional uplift during the

Quaternary, both along the platform and the coastal zone (Figs. 5 and 6). Pedoja *et al.* (2006a) proposed a 0.7-to-1 Ma age for the highest (360±10 m) marine terraces along the Coastal Cordillera and estimated an uplift rate around 0.3 to 0.5 $mm.yr^{-1}$ for the past 300 ka in the Manta Peninsula and La Plata Island. In the Santa Elena Peninsula, Cisneros Medina (2018) calculated a similar uplift between 0.3-0.4 $mm.yr^{-1}$ for terraces aging between 111-136 ka and 95-98 ka. These values are in accordance with Freisleben *et al.* (2021) who estimated a maximal uplift rate of 0.79 $mm.yr^{-1}$ in the Manta Peninsula and a minimal uplift rate of 0.07 mm/yr for <125 ka for marine terraces in the Santa Elena Peninsula. Although the coastal uplift is usually interpreted as a consequence of the Carnegie Ridge subduction (Cantalamessa and Di Celma, 2004; Pedoja *et al.*, 2006a and 2006b; Freisleben *et al.*, 2021), we also propose that the variation in vertical motions along the coast is due, at least partially, to deep crustal faults reactivation (*e.g.* Valdivia Fault Zone; Figs. 3 and 5). Therefore, marine terraces may not only express the effect of the forearc uplift in the Quaternary (*e.g.* Saillard *et al.*, 2017; Freisleben *et al.*, 2021), the effect of topographic asperities entering the subduction zone (Hsu, 1992; Macharé and Ortlieb, 1992; Saillard *et al.*, 2011; Hernández *et al.*, 2020; Freisleben *et al.*, 2021), and/or geometrical variations of the slab leading to subduction erosion and basal underplating (Saillard *et al.*, 2009). Instead, they may combine all these effects as a result of tectonic readjustments along reactivated faults.

7. Structural inheritance processes in subduction zones

Our study shows that the deformation of the southern Ecuadorian convergence margin can be ascribed to compressional, extensional and strike-slip tectonics overlapping in space and time since the Late Cretaceous (Fig. 5). The resultants are (1) the lateral growth of the forearc system due to oceanward tectonic collage, (2) the constant reorganisation of structural patterns due to fault reactivation, (3) the nature of the convergence margin as a function of interlinks between the upper plate and the subduction evolution, and (4) the influence of the deep forearc system on present-day deformation. This implies that crustal faults constantly interact over time, resulting in successive short- and/or long-spanning tectonic phases leading to the general growth of the accretionary wedge forming ahead a widening backstop. During this process, terranes stacked laterally the one another since the Late Cretaceous, and pre-existing crustal structures drove incipient strike-slip tectonics of the North Andean Sliver. Such structural inheritance, well-known in rift systems (*see* Schiffer *et al.* (2019) and references therein), remains poorly described in convergence settings due to constant erosion during the orogen organisation (*see* François *et al.* (2021) and references therein). Here, we discuss how such processes interact spatiotemporally and lead to the peculiar structural framework of the Santa Elena Peninsula region as part of the Ecuadorian margin.

7.1. The role of structural inheritance on long-lived subduction margin development

Due to the small amount of sediments at the trench, the overall Ecuadorian margin is classically considered as an erosional margin (Moberly *et al.*, 1982; Collot *et al.*, 2002 and 2008a; Sage *et al.*, 2006). In this model, only limited compressional deformation is observed in the frontal part of the margin where basins develop aside listric faults rooting on subhorizontal detachment levels. The resulting wedge morphology is controlled by a subduction channel, underplating and basal erosion. Many similar features are also observed in the Santa Elena Peninsula region, but thrusting appears to be the dominant deformation since the Late Cretaceous (Fig. 5). The long-lived compression likely produced constant folding of the old accretionary wedge. The top of this old accretionary wedge may correspond to an intra-crustal detachment controlling surficial normal faulting accommodation, as proposed by Collot *et al.* (2008). The resulting forearc growth requires constant tectonic readjustment with reactivation on the platform and/or destabilisation along the trench. In a certain way, this scenario follows the classical evolution of an accretionary wedge where the influence of old structures decreases in parallel of the backstop migration (Daly, 1989, Byrne *et al.*, 1993). Therefore, we propose that the accretionary wedge across the Santa Elena Peninsula region is produced in a dominant compression continuum, but its development self-maintains its dynamics with new fault formation together with fault rejuvenation.

Modern forearc systems may be classified depending on material transfers between converging plates and the long-term strain field (Noda, 2016; Noda and Miyakawa, 2017). Thus, a convergence margin is either accretionary or non-accretionary and the related forearc experiences compression or extension accordingly. Compressional accretionary-type margins are characterised by continentward-tilting strata and landward-migration of depocentres. Extensional accretionary margins develop normal faults due to the outer-wedge collapse. Non-accretionary margins have thin sediments at the trench and large and steady widths. Compressional-accretionary and extensional non-accretionary conditions are sometimes observed together in convergence settings like Chile (Polonia *et al.*, 2007; Contreras-Reyes *et al.*, 2010; Becerra *et al.*, 2013), the Cascadia (Trehu *et al.*, 1994; Gulick *et al.*, 2002; Booth-Rea *et al.*, 2008), Sumatra (Singh *et al.*, 2008, 2013, Shulgin *et al.*, 2013) or the Aleutian (Bruns *et al.*, 1987; Ryan and Scholl, 1989; von Huene *et al.*, 2012; Ryan *et al.*, 2012). Such characteristics are usually well-constrained for the modern forearc morphology but remain difficult to identify on a long timescale. Likewise, the forearc across the Santa Elena Peninsula region shows mixed characteristics and therefore cannot fulfil one category another. Instead, we propose that this part of the Ecuadorian margin switches from compressional to extensional/strike-slip regimes through time due to its long-lived evolution. Therefore, these transient variations are time dependent and explain the distribution of sedimentary sequences and the magnitude of bounding unconformities.

These variations also reinforce the hypotheses of large-scale segments along the modern Ecuadorian margin (Hernández *et al.*, 2020) and small-scale morphotectonic compartmentalisation (Freisleben *et al.*, 2021). These segments show a varying nature alongside, such as compressional accretionary in Columbia-Ecuador (López Ramos, 2009; Mantilla-Pimiento *et al.*, 2009), extensional non-accretionary in mid-Ecuador (Collot *et al.*, 2008a; Hernández *et al.*, 2020) and compression accretionary in northern Peru (von Huene *et al.*, 1996; Krabbenhöft *et al.*, 2004; Espurt *et al.*, 2018). These variations may express the buoyancy, the topography and the convergence direction of the subducting plate (Fig. 7), which, together with the amount of sediments deposited at the trench, directly control the forearc nature through long-lived compression. Large-scale subsidence and uplift are caused by the amount of basal erosion and the collision of asperities at the trench (von Huene and Scholl, 1991). Basal erosion, is not clearly observed from our seismic database but may occur along the Santa Elena Peninsula segment (Sage *et al.*, 2006; Collot *et al.*, 2011). Comparatively, enhanced erosion due to subducting asperities (Collot *et al.*, 2009; Proust *et al.*, 2016) largely influenced the morphology of the frontal part of the margin through tectonic reorganisation, since at least the Quaternary (Carnegie ridge subduction). This implies that the accretionary/non-accretionary character of the margin is also space dependent.

7.2. Implication of polyphase deformation relative to the margin seismic behaviour

Seismologically, the Ecuadorian margin is subdivided into several active segments based on historical large seismic ruptures and the interseismic coupling pattern on the plate interface (Nocquet *et al.*, 2014; Chlieh *et al.*, 2014, 2021; Gombert *et al.*, 2018; Vaca *et al.*, 2019). Collot *et al.* (2008b, 2017) proposed that subducting seamounts and ridges played an important role in the distribution of such variable seismic patterns along-strike the margin.

The Santa Elena Peninsula is above a low coupled interseismic coupled segment characterised by a very low level of seismic activity (Fig. 1b; Font *et al.*, 2013). The tectonic style of the Santa Elena Peninsula is not well established from the regional focal mechanism data (Dziewonski *et al.*, 1981; Ekström *et al.*, 2012; Vaca *et al.*, 2019). Very few focal mechanisms in the upper plate allow to characterize its tectonic regime. However, identified faulting pattern clearly shows that shortening is a dominant mechanism, at least in the upper crust (Fig. 5). Our study also suggests that the detachment fault zone is active over the Quaternary period although it is largely aseismic. This peculiar strain behaviour is probably due to the presence of lubricating fluids in the sedimentary column testified by bottom simulating reflectors (Fig. 5), that facilitate the reactivation of old faults trenchward. Therefore, such a type of aseismic deformation is influenced by the long-lasting structural evolution of the Santa Elena Peninsula region and is also intrinsically controlled by the tectonostratigraphy of the forearc.

8. Conclusion

The dynamics of the Santa Elena Peninsula forearc system is intimately linked to the long-lasting subduction of the Farallon/Nazca plates below South America since the Late Cretaceous. We show that the forearc sedimentation and regional unconformities are associated with crustal faults that progressively constructed a compressional margin through reactivation processes. Compression is intermittently perturbed by extension due to the progressive folding of an intra-Cenozoic crustal detachment running close to the top of the proposed basement since the Middle Eocene. This detachment also controls present-day gravitational movements in the frontal slope domain, that are probably facilitated by the presence of fluids. Finally, marine terraces show that the coastal deformation is dominated by active uplift related to the global convergence evolution.

The structural architecture of the Santa Elena Peninsula region suggests that tectonic reactivation processes play an important role during the long-lasting structural development of the margin. In particular, the successive compressional phases reflect the increasing stability of a backstop system that controlled in-sequence growth of an accretionary wedge. In addition, extension reflects long-term structural readjustments due to accretion and/or subduction, and middle-term uplift and/or gravitational collapse processes due to volume forces. Thus, we suggest that the pre-existing structural architecture of the upper plate is highly sensitive to varying boundary conditions at various time scales, leading to tectonic pulses taking place in a deformation continuum. This phenomenon of intermittent compression and extension may reflect, at least to a certain extent, a long-lasting segmentation of a subduction margin.

Acknowledgments

This study is part of the ANR MARACAS (ANR-18-CE31-0022) and was co-funded by the Institut de Recherche pour le Développement (IRD, France), Centre National de la Recherche Scientifique (CNRS, France) and Observatoire de la Côte d'Azur (OCA, France). Seismic lines and wireline data are kindly provided courtesy of Petroamazonas EP (https://www.petroamazonas.gob.ec/) and are published here for the first time. We are very grateful to the Editor Cristian Vallejo, and the three reviewers Etienne Jaillard and José Luis Granja Bruña and Carlos Aizprua for their very helpful comments during the review of the manuscript. Yvonne Font, Boris Marcaillou, Elia d'Acremont and Jean-Yves Collot are thanked for their constructive comments. In addition, Manuel Pubellier, Matthias Delescluse, Camille François and Laetitia Le Pourhiet are also thanked for background conversations about other subduction settings.

References

Aalto, K. R., and W. Miller (1999), Sedimentology of the Pliocene Upper Onzole Formation, an inner-trench slope succession in northwestern Ecuador, *Journal of South American Earth Sciences*, *12*(1), 69-85.

Aizprua, C., C. Witt, S. E. Johansen, and D. Barba (2019), Cenozoic Stages of Forearc Evolution Following the Accretion of a Sliver From the Late Cretaceous-Caribbean Large Igneous Province: SW Ecuador-NW Peru, *Tectonics*, *38*(4), 1441-1465.

Aizprua, C., C. Witt, J.-Y. Reynaud, M. Poujol, and D. Barba (2022), Comment on "The Chongón/Colonche orocline transrotational bending and the coeval opening of the Progreso basin in southwestern Ecuador" by Alemán et al, *Journal of South American Earth Sciences, 116*, 103714.

Alemán, A. M., A. A. Palencia, E. E. Lezama, and G. Montenegro (2021), The Chongón/Colonche orocline transrotational bending and the coeval opening of the Progreso basin in southwestern Ecuador, *Journal of South American Earth Sciences*, *111*, 103480.

Alvarado, A., L. Audin, J. M. Nocquet, E. Jaillard, P. Mothes, P. Jarrín, M. Segovia, F.

Rolandone, and D. Cisneros (2016), Partitioning of oblique convergence in the Northern Andes subduction zone: Migration history and the present-day boundary of the North Andean Sliver in Ecuador, *Tectonics*, *35*(5), 1048-1065.

Amórtegui, A., E. Jaillard, H. Lapierre, J.-E. Martelat, D. Bosch, and F. Bussy (2011), Petrography and geochemistry of accreted oceanic fragments below the Western Cordillera of Ecuador, *Geochemical Journal*, *45*(1), 57-78.

Armijo, R., and R. Thiele (1990), Active faulting in northern Chile: ramp stacking and lateral decoupling along a subduction plate boundary?, *Earth and Planetary Science Letters*, *98*(1), 40-61.

Audemard, F. E., and F. A. Audemard (2002), Structure of the Mérida Andes, Venezuela: relations with the South America–Caribbean geodynamic interaction, *Tectonophysics*, *345*(1), 1-26.

Azad, J. (1964), The Santa Elena Peninsula (Ecuador) a review of the Geology and prospects*Rep.*, AEO, Ancon.

Badley, M. E. (1985), *Practical seismic interpretation*, First ed., IHRDC Press, Boston, MA, United States.

Baize, S., L. Audin, A. Alvarado, H. Jomard, M. Bablon, J. Champenois, P. Espin, P. Samaniego, X. Quidelleur, and J.-L. Le Pennec (2020), Active Tectonics and Earthquake Geology Along the Pallatanga Fault, Central Andes of Ecuador, *Frontiers in Earth Science*, *8*(193).

Barckhausen, U., C. R. Ranero, S. C. Cande, M. Engels, and W. Weinrebe (2008), Birth of an intraoceanic spreading center, *Geology*, *36*(10), 767-770.

Beauval, C., H. Yepes, W. H. Bakun, J. Egred, A. Alvarado, and J.-C. Singaucho (2010), Locations and magnitudes of historical earthquakes in the Sierra of Ecuador (1587–1996), *Geophysical Journal International*, *181*(3), 1613-1633.

Beauval, C., H. Yepes, P. Palacios, M. Segovia, A. Alvarado, Y. Font, J. Aguilar, L. Troncoso, and S. Vaca (2013), An Earthquake Catalog for Seismic Hazard Assessment in Ecuador, *Bulletin of the Seismological Society of America*, *103*(2A), 773-786.

Becerra, J., E. Contreras-Reyes, and C. Arriagada (2013), Seismic structure and tectonics of the southern Arauco Basin, south-central Chile (~38°S), *Tectonophysics*, *592*, 53-66.

Benítez, S. B. (1995), Evolution géodynamique de la province côtière sud-équatorienne au Crétacé supèrieur-Tertiaire, PhD thesis, 127 pp, Université Joseph Fourier, Grenoble.

Benítez, S. B., M. Ronquillo, G. Montenegro, M. Ordóñez, and G. Toala (1986), Sintesis geológica de la cuenca Progreso Ecuador, in *4to Congresso Ecuatoriano de Geología, Minas y Petroleo*, edited, Quito, Ecuador.

Booth-Rea, G., D. Klaeschen, I. Grevemeyer, and T. Reston (2008), Heterogeneous deformation in the Cascadia convergent margin and its relation to thermal gradient (Washington, NW USA), *Tectonics*, *27*(4).

Bourgois, J., Y. Lagabrielle, P. DeWever, and E. Suess (1993), Tectonic history of the northern Peru convergent margin during the past 400 ka, *Geology*, *21*(6), 531-534.

Bourgois, J., F. Bigot-Cormier, D. Bourles, R. Braucher, O. Dauteuil, C. Witt, and F. Michaud (2007), Tectonic record of strain buildup and abrupt coseismic stress release across the northwestern Peru coastal plain, shelf, and continental slope during the past 200 kyr, *Journal of Geophysical Research: Solid Earth*, *112*(B4).

Brichau, S., P. Reyes, C. Gautheron, M. J. Hernández, F. Michaud, M. Leisen, A. Vacherat, M. Saillard, J. N. Proust, and P. O'Sullivan (2021), First timing constraints on the Ecuadorian

Coastal Cordillera exhumation: Geodynamic implications, *Journal of South American Earth Sciences*, *105*, 103007.

Bristow, C. R., and R. Hoffstetter (1977), *Ecuador. Lexique Stratigraphique International*, CNRS Publications, Paris.

Bruns, T. R., R.C.C. von Huene, S.D. Lewis, and J.W. Ladd (1987), Geology and petroleum potential of the Shumagin Margin, Alaska, in *Geology and Resource Potential of the Western North America and Adjacent Ocean Basins: Beaufort Sea to Baja California*, edited by D.W. Scholl, A. Grantz and J.G. Vedder, Earth Science Series 6, Circum-Pacific Council for Energy and Mineral Resources, Houston, Texas, pp. 157–189.

Byrne, D.E., W. Wang, and D.M. Davis (1993), Mechanical role of backstops in the growth of forearcs, *Tectonics*, *12*(1), 123-144.

Calahorrano Bétancourt, A. (2005), Structure de la marge du Golfe de Guayaquil (Equateur) et propriétés physiques du chenal de subduction, à partir de données de sismique marine réflexion et réfraction, 227 pp, Université Pierre et Marie Curie, Paris.

Cantalamessa, G., and C. Di Celma (2004), Origin and chronology of Pleistocene marine terraces of Isla de la Plata and of flat, gently dipping surfaces of the southern coast of Cabo San Lorenzo (Manabì, Ecuador), *Journal of South American Earth Sciences*, *16*(8), 633-648.

Cawood, P. A., A. Kröner, W. J. Collins, T. M. Kusky, W. D. Mooney, and B. F. Windley (2009), Accretionary orogens through Earth history, *Geological Society, London, Special Publications*, *318*, 1-36.

Chlieh, M., P.A. Mothes, J.M. Noquet, P. Jarrin, P. Charvis, D. Cisneros, Y. Font, J.Y. Collot, J.C. Villegas-Lanza, F. Roladone, M. Vallée, M. Regnier, M. Segovia, X. Martin, and Y. Yepes (2014), Distribution of discrete seismic asperities and aseismic slip along the Ecuadorian megathrust, *Earth and Planetary Science Letters*, *400*, 292-301.

Chlieh, M., C. Beauval, H. Yepes, J. Marinière, M. Saillard, and L. Audin (2021), Seismic and Aseismic Cycle of the Ecuador–Colombia Subduction Zone, *Frontiers in Earth Science*, *9*(685).

Cisneros Medina, A.L. (2018), Subduction versus crustal tectonic impact on the suthern Ecuadorian margin uplift : quantification of ulift rates and modelling of marine terraces, Master thesis, 38 pp, Université Grenoble Alpes, Grenoble.

Clift, P., and P. Vannucchi (2004), Controls on tectonic accretion versus erosion in subduction zones: Implications for the origin and recycling of the continental crust, *Reviews of Geophysics*, *42*(2).

Cobos Mite, L. E., and G. V. Montenegro (2010), Estudio integrado del golfo de Guayaquil del Mioceno al Reciente, 8pp, Escuela Politécnica del Litoral, Guayaquil.

Collot, J.-Y., P. Charvis, M.-A. Gutscher, and S. Operto (2002), Exploring the Ecuador-Colombia Active Margin and Interplate Seismogenic Zone, *Eos, Transactions American Geophysical Union*, *83*(17), 185-190.

Collot, J.-Y., W. Agudelo, A. Ribodetti, and B. Marcaillou (2008), Origin of a crustal splay fault and its relation to the seismogenic zone and underplating at the erosional north Ecuador–south Colombia oceanic margin, *Journal of Geophysical Research: Solid Earth*, *113*(B12).

Collot, J.-Y., A. Ribodetti, B. Marcaillou, and W. Agudelo (2008), Coeval subduction erosion and underplating associated with a crustal splay fault at the Ecuador-Colombia convergent margin, in *7th International Symposium on Andean Geodynamics - ISAG 2008*, edited, pp. 156-159, Nice.

Collot, J.-Y., F. Michaud, A. Alvarado, B. Marcaillou, M. Sosson, G. Ratzov, S. Migeon, A.

Calahorrano, and A. Pazmino (2009), Visión general de la morfología submarina del margen convergente de Ecuador-Sur de Colombia: implicaciones sobre la transferencia de masa y la edad de la subducción de la Cordillera de Carnegie, in *Geologia y Geofisica Marina y Terestre del Ecuador desde la costa continental hasta las islas Gapapagos*, edited by J. Y. Collot, V. Sallares and A. P. and, pp. 47-74, CNDM-INOCAR-IRD.

Collot, J.-Y., A. Ribodetti, W. Agudelo, and F. Sage (2011), The South Ecuador subduction channel: Evidence for a dynamic mega-shear zone from 2D fine-scale seismic reflection imaging and implications for material transfer, *Journal of Geophysical Research: Solid Earth*, *116*(B11).

Collot, J.-Y., E. Sanclemente, J.-M. Nocquet, A. Leprêtre, A. Ribodetti, P. Jarrin, M. Chlieh, D. Graindorge, and P. Charvis (2017), Subducted oceanic relief locks the shallow megathrust in central Ecuador, *Journal of Geophysical Research: Solid Earth*, *122*(5), 3286-3305.

Collot, J.-Y., G. Ratzov, P. Silva, J.-N. Proust, S. Migeon, M.-J. Hernández, F. Michaud, A. Pazmino, D. Barba Castillo, A. Alvarado, and S. Khurama, S. (2019), The Esmeraldas Canyon: A Helpful Marker of the Pliocene-Pleistocene Tectonic Deformation of the North Ecuador-Southwest Colombia Convergent Margin, *Tectonics*, *38*(8), 3140-3166.

Colman, J. A. R. (1970), Guidebook to the Geology of the Santa Elena Peninsula*Rep.*, 34 pp, Ecuadorian Geological and Geophysical Society, Quito.

Contreras-Reyes, E., E. R. Flueh, and I. Grevemeyer (2010), Tectonic control on sediment accretion and subduction off south central Chile: Implications for coseismic rupture processes of the 1960 and 2010 megathrust earthquakes, *Tectonics*, *29*(6).

Dahlen, F. A. (1990), Critical taper model of fold-and-thrust belts and accretionnary wedges, *Annual Review of Earth and Planetary Sciences*, *18*(1), 55-99.

Daly, M. C. (1989), Correlations between Nazca/Farallon Plate kinematics and forearc basin evolution in Ecuador, *Tectonics*, *8*(4), 769-790.

Delouis, B., H. Philip, L. Dorbath, and A. Cisternas (1998), Recent crustal deformation in the Antofagasta region (northern Chile) and the subduction process, *Geophysical Journal International*, *132*(2), 302-338.

Deniaud, Y. (2000), Enregistrements sédimentaire et structural de l'évolution géodynamique des Andes équatoriennes au cours du Néogène : étude des bassins d'avant-arc et bilans de masse.

Deniaud, Y., P. Baby, C. Basile, M. Ordonez, G. Montenegro, and G. Mascle (1999), Opening and tectonic and sedimentary evolution of the Gulf of Guayaquil: Neogene and Quaternary fore-arc basin of the south Ecuadorian Andes, *Comptes Rendus de l'Académie des Sciences - Series IIA - Earth and Planetary Science*, 181-187.

Dickinson, W. R., and D. R. Seely (1979), Structure and Stratigraphy of Forearc Regions, *AAPG Bulletin 63*(1), 2-31.

Dziewonski, A.M., Chou, T.-A., Woodhouse, J.H. (1981), Determination of earthquake source parameters from waveform data for studies of global and regional seismicity, *Journal of Geophysical Research: Solid Earth*, *86*, 2825-2852.

Dominguez, S., S. Lallemand, J. Malavieille, and R. von Huene (1998), Upper plate deformation associated with seamount subduction, *Tectonophysics*, *293*(3–4), 207-224.

Egbue, O., and J. Kellogg (2010), Pleistocene to Present North Andean “escape”, *Tectonophysics*, *489*(1), 248-257.

Egüez, A., M. Gaona, and A. Albán (2019), Mapa geologico de la Republica del Ecuador 2019.

Ekström, G., Nettles, M., Dziewoński, A.M. (2012), The global CMT project 2004–2010:

Centroid-moment tensors for 13,017 earthquakes, *Physics of the Earth and Planetary Interiors, 200-201*, 1-9.

Espurt, N., S. Brusset, P. Baby, P. Henry, M. Vega, Y. Calderon, L. Ramirez, and M. Saillard (2018), Deciphering the Late Cretaceous-Cenozoic Structural Evolution of the North Peruvian Forearc System, *Tectonics, 37*(1), 251-282.

Feininger, T., and C. R. Bristow (1980), Cretaceous and Paleogene geologic history of coastal Ecuador, *Geologische Rundschau, 69*(3), 849-874.

Fildani, A., A. M. Hessler, and S. A. Graham (2008), Trench-forearc interactions reflected in the sedimentary fill of Talara basin, northwest Peru, *Basin Research*, *20*(3), 305-331.

Font, Y., M. Segovia, S. Vaca, and T. Theunissen (2013), Seismicity patterns along the Ecuadorian subduction zone: new constraints from earthquake location in a 3-D a priori velocity model, *Geophysical Journal International*, *193*(1), 263-286.

François, C., M. Pubellier, C. Robert, C. Bulois, S. N. F. Jamaludin, R. Oberhänsli, M. Faure, M.R. St-Onge, and the IGCP Team (2021), Temporal and spatial evolution of orogens: a guide for geological mapping, *International Union of Geological Sciences*, *0*(0).

Freisleben, R., J. Jara-Muñoz, D. Melnick, J. M. Martínez, and M. R. Strecker (2021), Marine terraces of the last interglacial period along the Pacific coast of South America (1°N–40°S), *Earth Syst. Sci. Data*, *13*(6), 2487-2513.

Freymueller, J. T., J. N. Kellogg, and V. Vega (1993), Plate Motions in the north Andean region, *Journal of Geophysical Research: Solid Earth*, *98*(B12), 21853-21863.

Gombert, B., Z. Duputel, R. Jolivet, M. Simons, J. Jiang, C. Liang, E. J. Fielding, and L. Rivera (2018), Strain budget of the Ecuador–Colombia subduction zone: A stochastic view, *Earth and Planetary Science Letters*, *498*, 288-299.

Goossens, P. J., and W. I. Rose, JR. (1973), Chemical Composition and Age Determination of Tholeiitic Rocks in the Basic Igneous Complex, Ecuador, *GSA Bulletin*, *84*(3), 1043-1052.

Graindorge, D., A. Calahorrano, P. Charvis, J. Y. Collot, and N. Bethoux (2004), Deep structures of the Ecuador convergent margin and the Carnegie Ridge, possible consequence on great earthquake recurrence interval, *Geophysical Research Letters*, *31*(4), L04603 04601-04605.

Gulick, S. P. S., A. S. Meltzer, and S. H. Clarke (2002), Effect of the northward-migrating Mendocino triple junction on the Eel River forearc basin, California: Stratigraphic development, *GSA Bulletin*, *114*(2), 178-191.

Gutscher, M. A., and G. K. Westbrook (2009), Great Earthquakes in Slow-Subduction, Low-Taper Margins, in *Subduction Zone Geodynamics. Frontiers in Earth Sciences.*, edited by S. F. Lallemand, F., Springer, Berlin, Heidelberg.

Gutscher, M. A., J. Malavieille, S. Lallemand, and J. Y. Collot (1999), Tectonic segmentation of the North Andean margin: Impact of the Carnegie Ridge collision, *Earth and Planetary Science Letters*, *168*(3-4), 255-270.

Hamblin, W. K., and E.H. Christiansen (2004), *Earth's dynamic systems*, Prentice Hall, Pearson Education, Upper Saddle River, N.J.

Harpp, K. S., V. D. Wanless, R. H. Otto, K. Hornle, and R. Werner (2004), The Cocos and Carnegie Aseismic Ridges: a Trace Element Record of Long-term Plume–Spreading Center Interaction, *Journal of Petrology*, *46*(1), 109-133.

Hernández, M. J., F. Michaud, J.-Y. Collot, J.-N. Proust, and E. d'Acremont (2020), Evolution of the Ecuador offshore nonaccretionary-type forearc basin and margin segmentation, *Tectonophysics*, *781*, 228374.

Hey, R. (1977), Tectonic evolution of the Cocos-Nazca spreading center, *GSA Bulletin*, *88*(10), 1404-1420.

Hsu, J. T. (1992), Quaternary uplift of the Peruvian coast related to the subduction of the Nazca Ridge: 13.5 to 15.6 degrees south latitude, *Quaternary International*, *15-16*, 87-97.

Jaillard, E. (2022), Late Cretaceous-Paleogene orogenic build-up of the Ecuadorian Andes: Review and discussion, *Earth-Science Reviews*, *230*, 104033.

Jaillard, E., M. Ordoñez, S. B. Benitez, G. Berrones, N. Jiménez, G. Montenegro, and I. Zambrano (1995), Basin Development in an Accretionary, Oceanic-Floored Fore-Arc Setting: Southern Coastal Ecuador During Late Cretaceous-Late Eocene Time, in *Petroleum basins of South America*, edited by A. J. Tankard and R. W. Suarez, H.J., pp. 615-631, AAPG.

Jaillard, E., S. Benítez, and G. H. Mascle (1997), Palaeogene deformations of the forearc zone of south Ecuador in relation to the geodynamic evolution, *Bulletin de la Société Géologique de France*, *168*(4), 403-412.

Jaillard, E., M. Ordoñez, J. Suárez, J. Toro, D. Iza, and W. Lugo (2004), Stratigraphy of the late Cretaceous–Paleogene deposits of the cordillera occidental of central ecuador: geodynamic implications, *Journal of South American Earth Sciences*, *17*(1), 49-58.

Jaillard, E., P. Bengtson, M. Ordoñez, W. Vaca, A. Dhondt, J. Suárez, and J. Toro (2008), Sedimentary record of terminal Cretaceous accretions in Ecuador: The Yunguilla Group in the Cuenca area, *Journal of South American Earth Sciences*, *25*(2), 133-144.

Jaillard, E., H. Lapierre, M. Ordoñez, J. T. Álava, A. Amórtegui, J. Vanmelle, K. H. James, M. A. Lorente, and J. L. Pindell (2009), Accreted oceanic terranes in Ecuador: Southern edge of the Caribbean Plate?, in *The Origin and Evolution of the Caribbean Plate*, edited, p. 0, Geological Society of London.

Jiménez, N., and Mostajo, E. (1989), Zonación de nanofósiles calcâreos del Eoceno Punta Ancon-Punta Mambra, *Geociencias*, 24-29.

Kahrizi, A., M. Delescluse, N. Chamot-Rooke, M. Pubellier, A. Bécel, D.J. Shillington, M.R. Nedimovic, and C. Bulois (2023), Extensional forearc structures at the transition from Alaska to Aleutian Subduction Zone: slip partitioning, terranes and large earthquakes, *Comptes-Rendus de l'Académie des Sciences*.

Keller, G., T. Adatte, C. Hollis, M. Ordóñez, I. Zambrano, N. Jiménez, W. Stinnesbeck, A. Aleman, and W. Hale-Erlich (1997), The Cretaceous/Tertiary boundary event in Ecuador: reduced biotic effects due to eastern boundary current setting, *Marine Micropaleontology*, *31*(3-4), 97-133.

Kellog, J. N. V., V. (1995), Tectonic development of Panama, Costa Rica, and the Colombian Andes: Constraints from Global Positioning System geodetic studies and gravity, in *Geologic and Tectonic Development of the Caribbean Plate Boundary in Southern Central America*, edited by P. Mann, pp. 75-90, Geological Society of America, Boulder, Colorado.

Kerr, A. C., J. A. Aspden, J. Tarney, and L. F. Pilatasig (2002), The nature and provenance of accreted oceanic terranes in western Ecuador: geochemical and tectonic constraints, *Journal of the Geological Society*, *159*(5), 577-594.

Krabbenhöft, A., J. Bialas, H. Kopp, N. Kukowski, and C. Hübscher (2004), Crustal structure of the Peruvian continental margin from wide-angle seismic studies, *Geophysical Journal International*, *159*(2), 749-764.

Lallemand, S., P. Schnürle, and J. Malavieille (1994), Coulomb theory applied to accretionary and nonaccretionary wedges: Possible causes for tectonic erosion and/or frontal accretion, *Journal of Geophysical Research: Solid Earth*, *99*(B6), 12033-12055.

Le Pichon, X., P. Henry, and S. Lallemand (1993), Accretion and Erosion in Subduction Zones: The Role of Fluids, *Annual Review of Earth and Planetary Sciences*, *21*(1), 307-331.

Lonsdale, P. (1978), Ecuadorian subduction system, *AAPG Bull*, *62*(12), 2454-2477.

Lonsdale, P. (2005), Creation of the Cocos and Nazca plates by fission of the Farallon plate, *Tectonophysics*, *404*(3), 237-264.

Lonsdale, P., and K. D. Klitgord (1978), Structure and tectonic history of the eastern Panama Basin, *GSA Bulletin*, *89*(7), 981-999.

López Ramos, E. (2009), Évolution tectono-stratigraphique du double bassin avant-arc de la marge convergente Sud Colombienne-Nord Équatorienne pendant le Cénozoïque, PhD thesis, 371 pp, Université Nice Sophia Antipolis, Nice.

Loveless, J. P., G. D. Hoke, R. W. Allmendinger, G. González, B. L. Isacks, and D. A. Carrizo (2005), Pervasive cracking of the northern Chilean Coastal Cordillera: New evidence for forearc extension, *Geology*, *33*(12), 973-976.

Luzieux, L. D. A. (2007), Origin and late Cretaceous-Tertiary evolution of the Ecuadorian forearc, 204 pp, ETH Zürich, Zürich.

Luzieux, L. D. A., F. Heller, R. Spikings, C. F. Vallejo, and W. Winkler (2006), Origin and Cretaceous tectonic history of the coastal Ecuadorian forearc between 1°N and 3°S: Paleomagnetic, radiometric and fossil evidence, *Earth and Planetary Science Letters*, *249*(3), 400-414.

Macharé, J., and L. Ortlieb (1992), Plio-Quaternary vertical motions and the subduction of the Nazca Ridge, central coast of Peru, *Tectonophysics*, *205*(1), 97-108.

Mamberti, M. (2001), Origin and evolution of two distinct Cretaceous oceanic plateaus accreted in Western Ecuador (South America) : Petrological, geochemical and isotopic evidence, PhD thesis, 144 pp, Université Joseph-Fourier - Grenoble I, Grenoble.

Mantilla-Pimiento, A. M., G. Jentzsch, J. Kley, and C. Alfonso-Pava (2009), Configuration of the Colombian Caribbean Margin: Constraints from 2D Seismic Reflection data and Potential Fields Interpretation, Springer Berlin Heidelberg, Berlin, Heidelberg.

Martinod, J., L. Husson, P. Roperch, B. Guillaume, and N. Espurt (2010), Horizontal subduction zones, convergence velocity and the building of the Andes, *Earth and Planetary Science Letters*, *299*(3), 299-309.

Michaud, F., C. Witt, and J. Y. Royer (2009), Influence of the subduction of the Carnegie volcanic ridge on Ecuadorian geology: Reality and fiction, in *Memoir of the Geological Society of America*, edited, pp. 217-228.

Michaud, F., J.Y. Collot, G. Ratzov, J.N. Proust, A. Dano, J.F. Lebrun, M.J. Hernández, G. Loayza, A. Khaoulani, Y. Stoll, H. Pouderoux, and L. De Min (2018), A honeycomb seafloor morphology in carbonate sediment of the Carnegie Ridge (offshore Ecuador): Formation and potential geodynamic significance, *Geology*, *46*(11), 979-982.

Mitchum, R., P. Vail, and J. Sangree (1977), Seismic stratigraphy and global changes of sea level; Part 6, Stratigraphic interpretation of seismic reflection patterns in depositional sequences, in *Seismic Stratigraphy; Applications to Hydrocarbon Exploration*, edited by C. E. Payton, pp. 117–133, American Association of Petroleum Geologists.

Moberly, R., G. L. Shepherd, and W. T. Coulbourn (1982), Forearc and other basins, continental margin of northern and southern Peru and adjacent Ecuador and Chile, *Geological Society, London, Special Publications*, *10*(1), 171-189.

Moore, G. F., A. Taira, A. Klaus, L. Becker, B. Boeckel, B.A. Cragg, A. Dean, C.L. Fergusson, P. Henry, S. Hirano, T. Hisamitsu, S. Hunze, M. Kastner, A.J. Maltman, J.K.

Morgan, Y. Murakami, D.M. Saffer, M. Sánchez-Gómez, E.J. Screaton, D.C. Smith, A.J. Spivack, J. Steurer, H.J. Tobin, K. Ujiie, M.B. Underwood, and M. Wilson (2001), New insights into deformation and fluid flow processes in the Nankai Trough accretionary prism: Results of Ocean Drilling Program Leg 190, *Geochemistry, Geophysics, Geosystems, 2*(10).

Nocquet, J. M., J.C. Villegas-Lanza, M. Chlieh, P.A. Mothes, F. Rolandone, P. Jarrin, D. Cisneros, A. Alvarado, L. Audin, F. Bondoux, X. Martin, Y. Font, M. Régnier, M. Vallée, T. Tran, C. Beauval, J.M. Maguiña Mendoza, W. Martinez, H. Tavera, and H. Yepes, H. (2014), Motion of continental slivers and creeping subduction in the northern Andes, *Nature Geoscience, 7*(4), 287-291.

Nocquet, J. M., P. Jarrin, M. Vallée, P.A. Mothes, R. Grandin, F. Rolandone, B. Delouis, H. Yepes, F. Font, D. Fuentes, M. Régnier, A. Laurendeau, D. Cisneros, S. Hernandez, A. Sladen, J.C. Singaucho, H. Mora, J. Gomez, L. Montes, and P. Charvis, (2017), Supercycle at the Ecuadorian subduction zone revealed after the 2016 Pedernales earthquake, *Nature Geoscience, 10*(2), 145-149.

Noda, A. (2016), Forearc basins: Types, geometries, and relationships to subduction zone dynamics, *Geological Society of America Bulletin, 128*(5-6), 879-895.

Noda, A., and A. Miyakawa (2017), Deposition and Deformation of Modern Accretionary-Type Forearc Basins: Linking Basin Formation and Accretionary Wedge Growth, in *Evolutionary Models of Convergent Margins - Origin of Their Diversity*, edited by Y. Itoh, IntechOpen.

Norabuena, E. O., T. H. Dixon, S. Stein, and C. G. A. Harrison (1999), Decelerating Nazca-South America and Nazca-Pacific Plate motions, *Geophysical Research Letters, 26*(22), 3405-3408.

Ordóñez, M., N. Jiménez, and J. Suarez (2006), Micropaleontologia ecuatoriana : Datos bioestratigráficos y paleoecológicos de las cuencas: Graben de Jambelí. Progreso. Manabí, Esmeraldas y Oriente; del levantamiento de la Península de Santa Elena, y de las cordilleras colonche, costera y occidental, *Petroproducción, Quito*, 1-633.

Pardo-Casas, F., and P. Molnar (1987), Relative motion of the Nazca (Farallon) and South American Plates since Late Cretaceous time, *Tectonics*, *6*(3), 233-248.

Pedoja, K., J. F. Dumont, M. Lamothe, L. Ortlieb, J. Y. Collot, B. Ghaleb, M. Auclair, V. Alvarez, and B. Labrousse (2006a), Plio-Quaternary uplift of the Manta Peninsula and La Plata Island and the subduction of the Carnegie Ridge, central coast of Ecuador, *Journal of South American Earth Sciences, 22*(1-2), 1-21.

Pedoja, K., L. Ortlieb, J. F. Dumont, M. Lamothe, B. Ghaleb, M. Auclair, and B. Labrousse (2006b), Quaternary coastal uplift along the Talara Arc (Ecuador, Northern Peru) from new marine terrace data, *Marine Geology, 228*(1-4), 73-91.

Pennington, W. D. (1981), Subduction of the eastern Panama basin and seismotectonics of northwestern South America, *Journal of Geophysical Research*, *86*(B11), 10753-10770.

Pilger, R. H. (1984), Cenozoic plate kinematics, subduction and magmatism: South American Andes, *Journal of the Geological Society*, *141*(5), 793-802.

Polonia, A., L. Torelli, G. Brancolini, and M.-F. Loreto (2007), Tectonic accretion versus erosion along the southern Chile trench: Oblique subduction and margin segmentation, *Tectonics*, *26*(3).

Proust, J. N., C. Martillo, F. Michaud, J. Y. Collot, and O. Dauteuil (2016), Subduction of seafloor asperities revealed by a detailed stratigraphic analysis of the active margin shelf sediments of Central Ecuador, *Marine Geology, 380*, 345-362.

Quinteros, J., and S. V. Sobolev (2013), Why has the Nazca plate slowed since the Neogene?, *Geology*, *41*(1), 31-34.

Ranero, C. R., and R. von Huene (2000), Subduction erosion along the Middle America convergent margin, *Nature*, *404*(6779), 748-752.

Ratzov, G., M. Sosson, J.-Y. Collot, and S. Migeon (2012), Late Quaternary geomorphologic evolution of submarine canyons as a marker of active deformation on convergent margins: The example of the South Colombian margin, *Marine Geology*, *315-318*, 77-97.

Reyes, P. (2013), Évolution du relief le long des marges actives : étude de la déformation Plio-Quaternaire de la cordillère côtière d'Équateur, PhD Thesis thesis, 312 pp, Université Nice Sophia Antipolis.

Reyes, P., and F. Michaud (2012), *Mapa Geologica de la margen costera ecuatoriana (1 :500000)*.

Reynaud, C., É. Jaillard, H. Lapierre, M. Mamberti, and G. H. Mascle (1999), Oceanic plateau and island arcs of southwestern Ecuador: their place in the geodynamic evolution of northwestern South America, *Tectonophysics*, *307*(3), 235-254.

Roperch, P., F. Mégard, C. Laj, T. Mourier, T. M. Clube, and C. Noblet (1987), Rotated oceanic blocks in western Ecuador, *Geophysical Research Letters*, *14*(5), 558-561.

Ryan, H. F., and D. W. Scholl (1989), The evolution of forearc structures along an oblique convergent margin, central Aleutian Arc, *Tectonics*, *8*(3), 497-516.

Ryan, H. F., A. E. Draut, K. Keranen, and D. W. Scholl (2012), Influence of the Amlia fracture zone on the evolution of the Aleutian Terrace forearc basin, central Aleutian subduction zone, *Geosphere*, *8*(6), 1254-1273.

Sage, F., J.-Y. Collot, and C. R. Ranero (2006), Interplate patchiness and subduction-erosion mechanisms: Evidence from depth-migrated seismic images at the central Ecuador convergent margin, *Geology*, *34*(12), 997-1000.

Saillard, M., S. R. Hall, L. Audin, D. L. Farber, G. Hérail, J. Martinod, V. Regard, R. C. Finkel, and F. Bondoux (2009), Non-steady long-term uplift rates and Pleistocene marine terrace development along the Andean margin of Chile (31°S) inferred from 10Be dating, *Earth and Planetary Science Letters*, *277*(1), 50-63.

Saillard, M., S. R. Hall, L. Audin, D. L. Farber, V. Regard, and G. Hérail (2011), Andean coastal uplift and active tectonics in southern Peru: 10Be surface exposure dating of differentially uplifted marine terrace sequences (San Juan de Marcona, ~15.4°S), *Geomorphology*, *128*(3), 178-190.

Saillard, M., L. Audin, B. Rousset, J.-P. Avouac, M. Chlieh, S. R. Hall, L. Husson, and D. L. Farber (2017), From the seismic cycle to long-term deformation: linking seismic coupling and Quaternary coastal geomorphology along the Andean megathrust, *Tectonics*, *36*(2), 241-256.

Sallarès, V., and P. Charvis (2003), Crustal thickness constraints on the geodynamic evolution of the Galapagos Volcanic Province, *Earth and Planetary Science Letters*, *214*(3), 545-559.

Sallarès, V., and C. R. Ranero (2005), Structure and tectonics of the erosional convergent margin off Antofagasta, north Chile (23°30′S), *Journal of Geophysical Research: Solid Earth*, *110*(B6).

Schiffer, C., A.G. Doré, G.R. Foulger, D. Franke, L. Geoffroy, L. Gernigon, B. Holdsworth, N. Kusznir, E. Lundin, K. McCaffrey, A.L. Peace, K.D. Petersen, T.B. Phillips, R. Stephenson, M.S. Stoker, and K. Welford (2020), Structural inheritance in the North Atlantic, *Earth-Science*

Reviews, *206*, 102975.

Schütte, P., M. Chiaradia, and B. Beate (2010), Geodynamic controls on Tertiary arc magmatism in Ecuador: Constraints from U–Pb zircon geochronology of Oligocene–Miocene intrusions and regional age distribution trends, *Tectonophysics*, *489*(1), 159-176.

Séranne, M. (1987), Evolution tectono-sédimentaire du bassin de Talara (nord-ouest du Pérou), *Bulletin de l'Institut francais d'études Andins*.

Serra, O. (1979), *Diagraphies différées: Acquisition des données diagraphiques*, Elf-Aquitaine.

Serra, O. (1985), *Diagraphies différées: bases de l'interprétation*, Elf-Aquitaine.

Seton, M., R.D. Müller, S. Zahirovic, C. Gaina, Z. Torsvik, G. Shephard, A. Talsma, M. Gurnis, M. Turner, S. Maus, and M. Chandler (2012), Global continental and ocean basin reconstructions since 200 Ma, *Earth-Science Reviews*, *113*, 212-270.

Seyler, M., C. Witt, B. Omaña, C. Durand, M. Chiaradia, D. Villagomez, and M. Poujol (2021), Late Cretaceous felsic intrusions in oceanic plateau basalts in SW Ecuador: Markers of subduction initiation?, *Journal of South American Earth Sciences*, *110*, 103348.

Shulgin, A., H. Kopp, D. Klaeschen, C. Papenberg, F. Tilmann, E. R. Flueh, D. Franke, U. Barckhausen, A. Krabbenhoeft, and Y. Djajadihardja (2013), Subduction system variability across the segment boundary of the 2004/2005 Sumatra megathrust earthquakes, *Earth and Planetary Science Letters*, *365*, 108-119.

Singh, S. C., H. Carton, P. Tapponnier, N.D. Hananto, A.P.S. Chauhan, D. Hartoyo, M. Bayly, S. Moeljopranoto, T. Bunting, P. Christie, H. Lubis, and J. Martin, (2008), Seismic evidence for broken oceanic crust in the 2004 Sumatra earthquake epicentral region, *Nature Geoscience*, *1*(11), 777-781.

Singh, S. C., R. Moeremans, J. McArdle, and K. Johansen (2013), Seismic images of the sliver strike-slip fault and back thrust in the Andaman-Nicobar region, *Journal of Geophysical Research: Solid Earth*, *118*(10), 5208-5224.

Siravo, G., F. Speranza, M. Mulas, and V. Costanzo-Alvarez (2021), Significance of Northern Andes Terrane Extrusion and Genesis of the Interandean Valley: Paleomagnetic Evidence From the "Ecuadorian Orocline", *Tectonics*, *40*(7), e2020TC006684.

Somoza, R., and M. E. Ghidella (2012), Late Cretaceous to recent plate motions in western South America revisited, *Earth and Planetary Science Letters*, *331-332*, 152-163.

Spikings, R. A., W. Winkler, D. Seward, and R. Handler (2001), Along-strike variations in the thermal and tectonic response of the continental Ecuadorian Andes to the collision with heterogeneous oceanic crust, *Earth and Planetary Science Letters*, *186*(1), 57-73.

Steinmann, M., D. Hungerbühler, D. Seward, and W. Winkler (1999), Neogene tectonic evolution and exhumation of the southern Ecuadorian Andes: a combined stratigraphy and fission-track approach, *Tectonophysics*, *307*(3), 255-276.

Stern, R., J. (2002), Subduction zones, *Reviews of Geophysics*, *40*(4), 3-1, 3-38.

Tebbens, S. F., and S. C. Cande (1997), Southeast Pacific tectonic evolution from Early Oligocene to Present, *Journal of Geophysical Research: Solid Earth*, *102*(B6), 12061-12084.

Trehu, A. M., I. Asudeh, T. M. Brocher, J. H. Luetgert, M. W.D., J. L. Nabelek, and Y. Nakamura (1994), Crustal Architecture of the Cascadia Forearc, *Science*, *266*(5183), 237-243.

Trenkamp, R., J. N. Kellogg, J. T. Freymueller, and H. P. Mora (2002), Wide plate margin deformation, southern Central America and northwestern South America, CASA GPS observations, *Journal of South American Earth Sciences*, *15*(2), 157-171.

Vaca, S., M. Vallée, J.-M. Nocquet, and A. Alvarado (2019), Active deformation in Ecuador enlightened by a new waveform-based catalog of earthquake focal mechanisms, *Journal of South American Earth Sciences*, *93*, 449-461.

Vail, P. R., R.M. Mitchum, and S. I. Thompson (1977), Seismic Stratigraphy and Global Changes of Sea Level, Part 3: Relative Changes of Sea Level from Coastal Onlap, in *Seismic stratigraphy - applications to hydrocarbon exploration*, edited by C. E. Clayton, pp. 63-81, American Association of Petroleum Geologists Memoir

Vallejo, C., W. Winkler, R. A. Spikings, L. Luzieux, F. Heller, F. Bussy, S. M. Kay, V. A. Ramos, and W. R. Dickinson (2009), Mode and timing of terrane accretion in the forearc of the Andes in Ecuador, in *Backbone of the Americas: Shallow Subduction, Plateau Uplift, and Ridge and Terrane Collision*, edited, p. 0, Geological Society of America.

Vallejo, C., Soria, F., Tornos, F., Naranjo, G., Rosero, B., Salazar, F., Cochrane, R., 2016. Geology of El Domo deposit in central Ecuador: a VMS formed on top of an accreted margin. *Mineralium Deposita*, 51, 389-409.

Vallejo, C., Spikings, R.A., Horton, B.K., Luzieux, L., Romero, C., Winkler, W., Thomsen, T.B. (2019). Chapter 8 - Late Cretaceous to Miocene stratigraphy and provenance of the coastal forearc and Western Cordillera of Ecuador: Evidence for accretion of a single oceanic plateau fragment, in *Andean Tectonics*, edited by B.K. Horton and A. Folguera, pp. 209-236, Elsevier.

van Melle, J., W. Vilema, B. Faure-Brac, M. Ordoñez, H. Lapierre, N. Jimenez, E. Jaillard, and M. Garcia (2008), Pre-collision evolution of the Piñón oceanic terrane of SW Ecuador: stratigraphy and geochemistry of the "Calentura Formation", *Bulletin de la Société Géologique de France*, *179*(5), 433-443.

Vannucchi, P., D. M. Fisher, S. Bier, and T. W. Gardner (2006), From seamount accretion to tectonic erosion: Formation of Osa Mélange and the effects of Cocos Ridge subduction in southern Costa Rica, *Tectonics*, *25*(TC2004).

Vannucchi, P., F. Remitti, and G. Bettelli (2008), Geological record of fluid flow and seismogenesis along an erosive subducting plate boundary, *Nature*, *451*(7179), 699-703.

Vannucchi, P., F. Sage, J. Phipps Morgan, F. Remitti, and J.-Y. Collot (2012), Toward a dynamic concept of the subduction channel at erosive convergent margins with implications for interplate material transfer, *Geochemistry, Geophysics, Geosystems*, *13*(2).

Veliz-Borel, V., V. Mouslopoulou, A. Nicol, J. Begg, and O. Oncken (2022), Normal Faulting along the Kythira-Antikythira Strait, Southwest Hellenic Forearc, Greece, *Frontiers in Earth Science*, *9*.

Villegas-Lanza, J. C., M. Chlieh, O. Cavalié, H. Tavera, P. Baby, J. Chire-Chira, and J.-M. Nocquet (2016), Active tectonics of Peru: Heterogeneous interseismic coupling along the Nazca megathrust, rigid motion of the Peruvian Sliver, and Subandean shortening accommodation, *Journal of Geophysical Research: Solid Earth*, *121*(10), 7371-7394.

von Huene, R., and S. Lallemand (1990), Tectonic erosion along the Japan and Peru convergent margins, *GSA Bulletin*, *102*(6), 704-720.

von Huene, R., and D. W. Scholl (1991), Observations at convergent margins concerning sediment subduction, subduction erosion, and the growth of continental crust, *Reviews of Geophysics*, *29*(3), 279-316.

von Huene, R., I. A. Pecher, and M.-A. Gutscher (1996), Development of the accretionary prism along Peru and material flux after subduction of Nazca Ridge, *Tectonics*, *15*(1), 19-33.

von Huene, R., W. Weinrebe, and F. Heeren (1999), Subduction erosion along the North Chile margin, *Journal of Geodynamics*, *27*(3), 345-358.

von Huene, R., C. R. Ranero, and P. Vannucchi (2004), Generic model of subduction erosion, *Geology*, *32*(10), 913-916.

von Huene, R., J. J. Miller, and W. Weinrebe (2012), Subducting plate geology in three great earthquake ruptures of the western Alaska margin, Kodiak to Unimak, *Geosphere*, *8*(3), 628-644.

Wang, K., Y. Hu, R. von Huene, and N. Kukowski (2010), Interplate earthquakes as a driver of shallow subduction erosion, *Geology*, *38*(5), 431-434.

White, S. M., R. Trenkamp, and J. N. Kellogg (2003), Recent crustal deformation and the earthquake cycle along the Ecuador–Colombia subduction zone, *Earth and Planetary Science Letters*, *216*(3), 231-242.

Witt, C., and J. Bourgois (2010), Forearc basin formation in the tectonic wake of a collision-driven, coastwise migrating crustal block: The example of the North Andean block and the extensional Gulf of Guayaquil-Tumbes Basin (Ecuador-Peru border area), *GSA Bulletin*, *122*(1-2), 89-108.

Witt, C., J. Bourgois, F. Michaud, M. Ordoñez, N. Jiménez, and M. Sosson (2006), Development of the Gulf of Guayaquil (Ecuador) during the Quaternary as an effect of the North Andean block tectonic escape, *Tectonics*, *25*(3).

Witt, C., J. Y. Reynaud, D. Barba, M. Poujol, C. Aizprua, M. Rivadeneira, and C. Amberg (2019), From accretion to forearc basin initiation: The case of SW Ecuador, Northern Andes, *Sedimentary Geology*, *379*, 138-157.

Yáñez, G., and J. Cembrano (2004), Role of viscous plate coupling in the late Tertiary Andean tectonics, *Journal of Geophysical Research: Solid Earth*, *109*(B2).

Fig. 1: Geodynamics of the western margin of Ecuador. (a) Geodynamic setting of Ecuador in the context of the eastern Pacific subduction. Velocity vectors represent the plate motion of the Nazca Plate (NAZ) compare to the South America Plate (SAM) (Trenkamp *et al.*, 2002), and the relative North Andean Sliver (NAS) and Inca Sliver (INS) motions compare to the Nazca Plate and South America Plate (Nocquet *et al.*, 2014). Velocities are in mm/yr. Yellow stars show historical megathrust earthquakes along the subduction zone (Nocquet *et al.*, 2016). (b) Structural map of the southwestern margin of Ecuador (adapted from Reyes and Michaud, 2012). The interseismic coupling contouring is adapted from Nocquet *et al.* (2014). PPF: Puná-Pallatanga Fault. LCF: La Cruz Fault. CCF : Chogon-Colonche Fault. JIF: Jipijapa Fault. JAF: Jama Fault. CAF: Canande Fault.

Fig. 2: Simplified stratigraphy and Formation/Group of the Santa Elena Province region. The stratigraphic column is principally based on lithological descriptions of Benítez (1995), Jaillard *et al.* (1995, 2009), Reyes and Michaud (2017), Egüez *et al.* (2017), and Jaillard (2022). Regional tectonic episodes principally described onshore are indicated. Major unconformities are also indicated.

Fig. 3: Map of available subsurface data in the study area (*see* location on Fig. 1b). The base map corresponds to long-wavelength free air gravity data and high-resolution aero-gravity data (Hernández *et al.*, 2020). The framework of Cenozoic to present-day faults of the Valdivia Basin-Santa Elena Peninsula region and northern edge of the Progreso Basin was constrained by seismic reflection profiles (thin grey lines). Only faults recognised on more than two consecutive seismic lines are indicated. Onshore faults are also derived from Reyes and Michaud (2017). Locations of wells B1-NSXI-1X (*see* interpretation on Fig. 4) and B1-MT1-1X, as well as the composite onshore-offshore seismic profile across the Santa Elena Peninsula forearc (*see* interpretation on Fig. 5) are shown.

Fig. 4: Interpreted stratigraphy in Well B1-NSXI-1X (gamma ray (GR) and sonic logs) and correlation with field data. Ages are interpreted according to Benítez (1995), Deniaud (2000), Jaillard *et al.* (1995, 2009), Luzieux *et al.* (2007), Reyes (2013), Reyes and Michaud (2012), Ergüez *et al.* (2017), and Jaillard (2022). Major unconformities are also indicated. This well is used to calibrate the offshore seismic profile MR08-756 (Fig. 5).

Fig. 5: Seismic interpretation of the Santa Elena Peninsula region. (a) Interpretation of composite seismic profile across the Santa Elena Peninsula region, calibrated using surface data and Well B1-NSXI-1X. (b) Schematic cross-section based on the seismic interpretation as described in the text. Labels of seismic lines are indicated. The location of the profile is shown

on Figs. 1 and 3. Seismic profiles without and with interpretation are shown on Annexes 1 and 2. BSR: Bottom simulating reflector.

Fig. 6: Marine terraces at Punta Salinas, La Chocolatera, in the westernmost part of the Santa Elena Peninsula region. See location on Fig. 3. A sequence of four marine terraces can be seen: a sharp shore platform (T1), probably Holocene in age, that stands between the present-day sea level and the 18±2 m terrace (T2), the T3 marine terrace at 48±2 m and the T4 terrace whose shoreline angle is at more than 80 m (Pedoja *et al.*, 2006a). The T2 and T3 terraces are assigned to the MIS 5e (~125 ka) and the MIS 9 or 11 by Pedoja *et al.* (2006a).

Fig. 7: Convergence rate (Somoza and Guidella, 2012) and direction along the Farallon/Nazca (Pardo-Casas and Molnar, 1987) subduction throughout the Cenozoic. Grey areas indicate the uncertainty limits. Major unconformities as defined in the study are indicated on the figure but note that their ages are only indicative due to age bias along each surface. See Fig. 2 for color references of the simplified stratigraphy.

Annexes:

Annexe 1: Onshore seismic lines B90-50 and B90-46 without (a) and with (b) interpretation.

Annexe 2: Offshore seismic lines MR08-756 and E86-183B without (a) and with (b) interpretation.

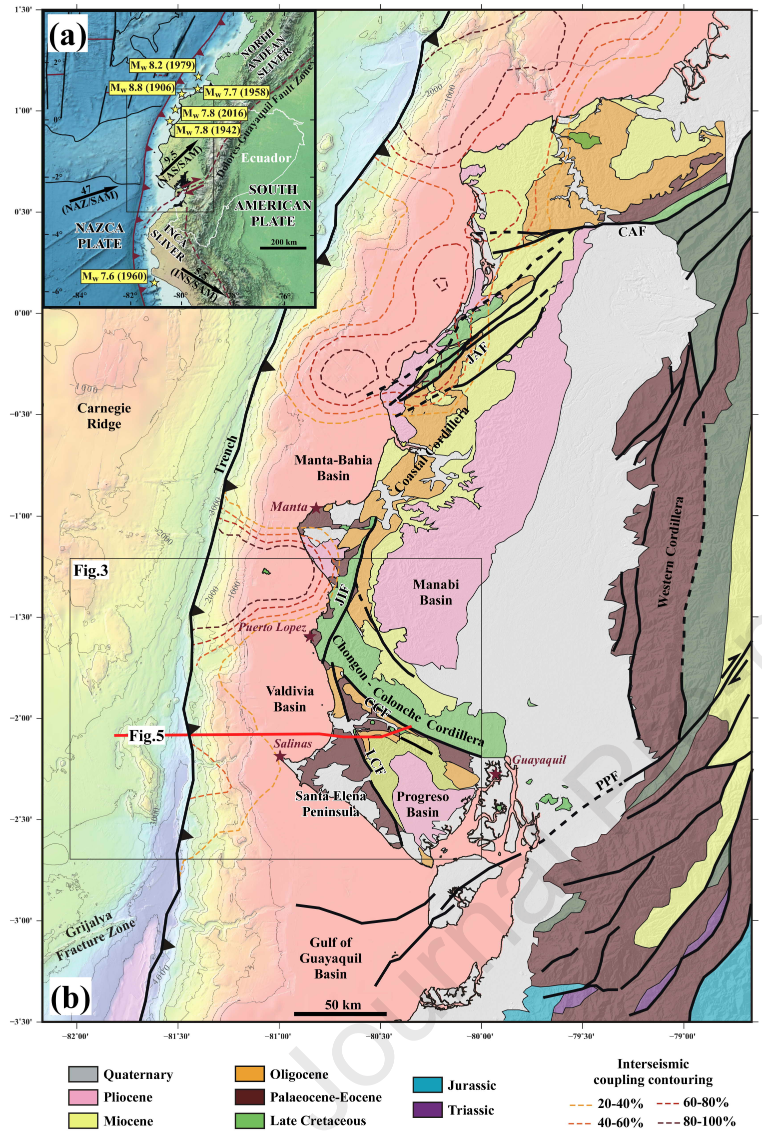
(a)
NORTH ANDEAN SLIVER
Mw 8.2 (1979)
Mw 8.8 (1906)
Mw 7.7 (1958)
Mw 7.8 (2016)
Mw 7.8 (1942)
Dolores-Guayaquil Fault Zone
Ecuador
9.5 (NAS/SAM)
47 (NAZ/SAM)
SOUTH AMERICAN PLATE
NAZCA PLATE
INCA SLIVER
5.5 (INS/SAM)
200 km
Mw 7.6 (1960)
(b)
CAF
JAF
Carnegie Ridge
Trench
Manta-Bahia Basin
Coastal Cordillera
Manta
Fig.3
JJF
Manabi Basin
Western Cordillera
Puerto Lopez
Chongon - Colonche Cordillera
Valdivia Basin
CCF
Fig.5
Salinas
LCF
Guayaquil
PPF
Santa-Elena Peninsula
Progreso Basin
Grijalva Fracture Zone
Gulf of Guayaquil Basin
50 km
Quaternary
Pliocene
Miocene
Oligocene
Palaeocene-Eocene
Late Cretaceous
Jurassic
Triassic
Interseismic coupling contouring
20-40%
40-60%
60-80%
80-100%

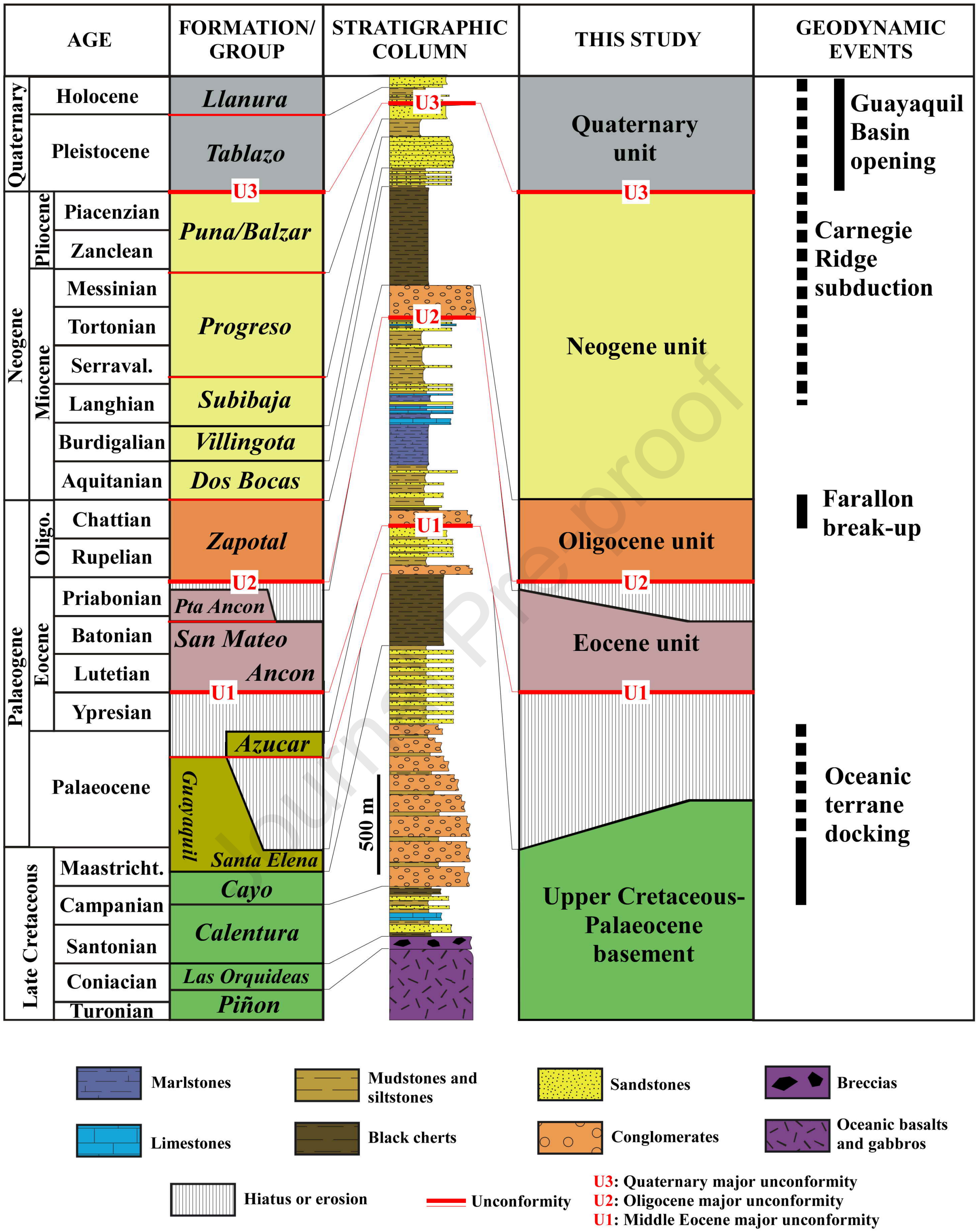
AGE
FORMATION/ GROUP
STRATIGRAPHIC COLUMN
THIS STUDY
GEODYNAMIC EVENTS
Quaternary
Holocene
Pleistocene
Neogene
Pliocene
Piacenzian
Zanclean
Miocene
Messinian
Tortonian
Serraval.
Langhian
Burdigalian
Aquitanian
Palaeogene
Oligo.
Chattian
Rupelian
Eocene
Priabonian
Batonian
Lutetian
Ypresian
Palaeocene
Late Cretaceous
Maastricht.
Campanian
Santonian
Coniacian
Turonian
Llanura
Tablazo
Puna/Balzar
Progreso
Subibaja
Villingota
Dos Bocas
Zapotal
Pta Ancon
San Mateo
Ancon
Azucar
Guayaquil
Santa Elena
Cayo
Calentura
Las Orquideas
Piñon
U3
U2
U1
500 m
Quaternary unit
Neogene unit
Oligocene unit
Eocene unit
Upper Cretaceous-Palaeocene basement
Guayaquil Basin opening
Carnegie Ridge subduction
Farallon break-up
Oceanic terrane docking
Marlstones
Mudstones and siltstones
Sandstones
Breccias
Limestones
Black cherts
Conglomerates
Oceanic basalts and gabbros
Hiatus or erosion
Unconformity
U3: Quaternary major unconformity
U2: Oligocene major unconformity
U1: Middle Eocene major unconformity

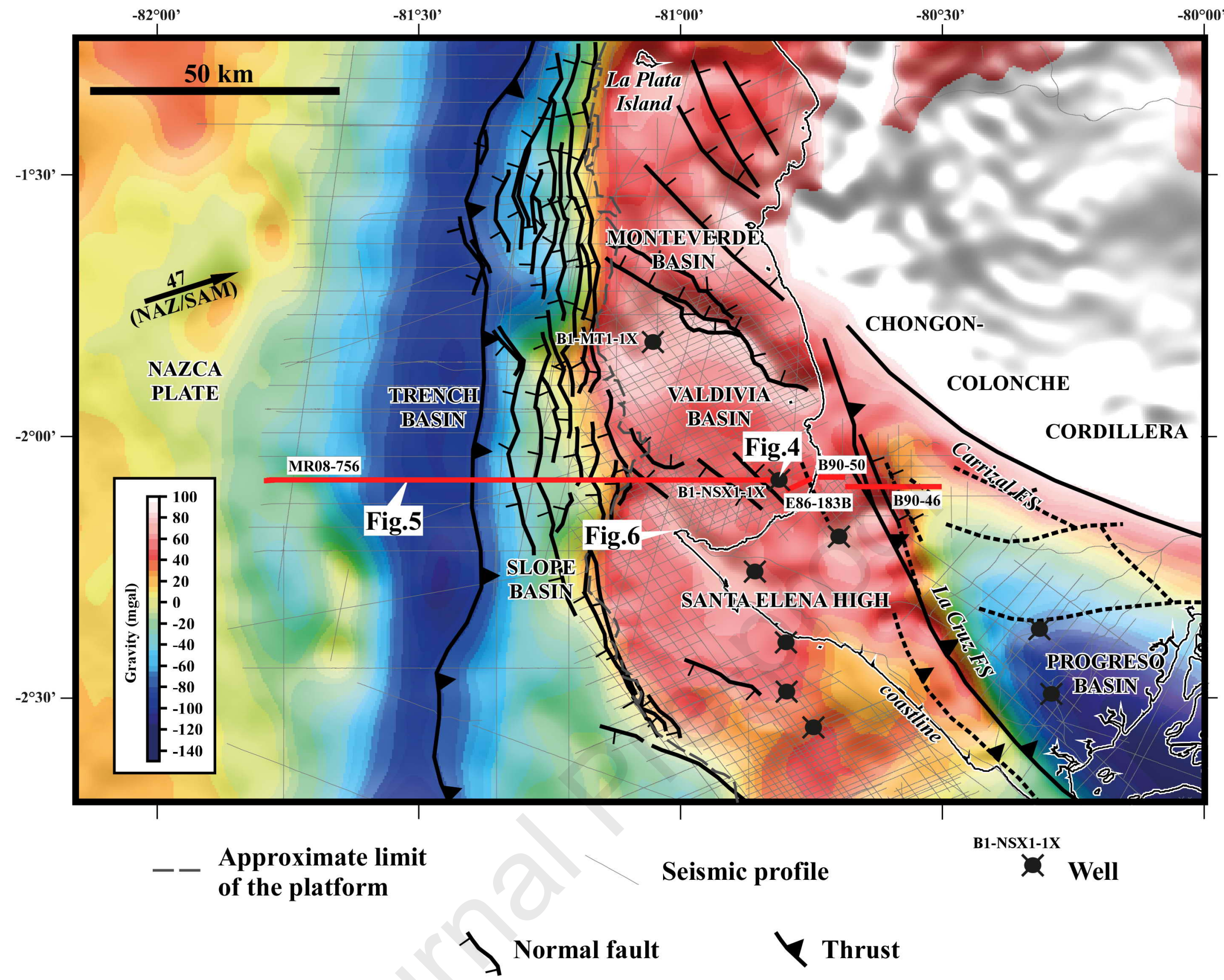
-82°00'
-81°30'
-81°00'
-80°30'
-80°00'
-1°30'
-2°00'
-2°30'
50 km
La Plata Island
47 (NAZ/SAM)
NAZCA PLATE
TRENCH BASIN
SLOPE BASIN
MONTEVERDE BASIN
VALDIVIA BASIN
SANTA ELENA HIGH
CHONGON-
COLONCHE
CORDILLERA
PROGRESO BASIN
Carrizal FS
La Cruz FS
coastline
B1-MT1-1X
MR08-756
Fig.5
Fig.4
Fig.6
B90-50
B1-NSX1-1X
E86-183B
B90-46
Gravity (mgal)
100
80
60
40
20
0
-20
-40
-60
-80
-100
-120
-140
Approximate limit of the platform
Seismic profile
B1-NSX1-1X
Well
Normal fault
Thrust

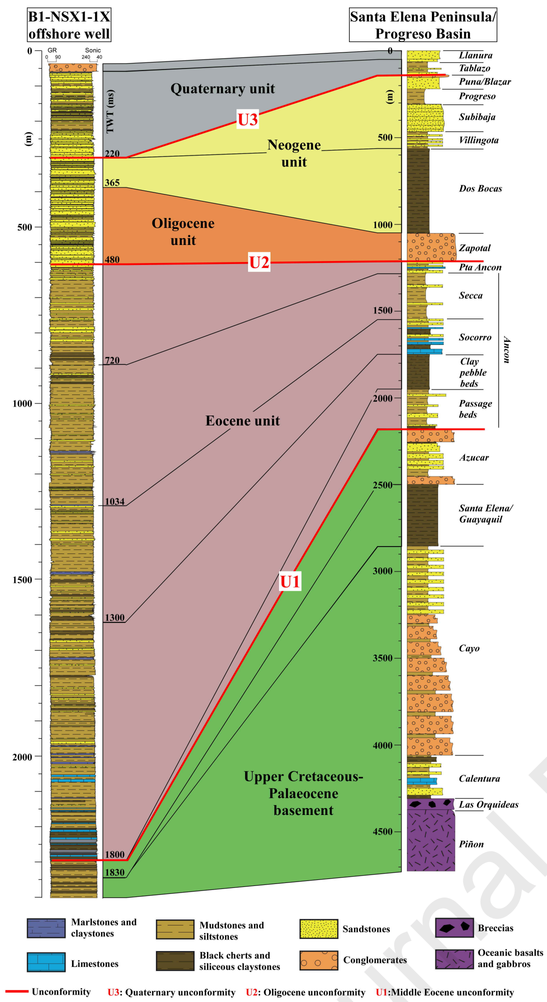

B1-NSX1-1X offshore well
Santa Elena Peninsula/ Progreso Basin
GR
Sonic
TWT (ms)
(m)
Quaternary unit
Neogene unit
Oligocene unit
Eocene unit
Upper Cretaceous-Palaeocene basement
U3
U2
U1
Llanura
Tablazo
Puna/Blazar
Progreso
Subibaja
Villingota
Dos Bocas
Zapotal
Pta Ancon
Secca
Socorro
Clay pebble beds
Passage beds
Ancon
Azucar
Santa Elena/ Guayaquil
Cayo
Calentura
Las Orquideas
Piñon
Marlstones and claystones
Mudstones and siltstones
Sandstones
Breccias
Limestones
Black cherts and siliceous claystones
Conglomerates
Oceanic basalts and gabbros
Unconformity
U3: Quaternary unconformity
U2: Oligocene unconformity
U1:Middle Eocene unconformity

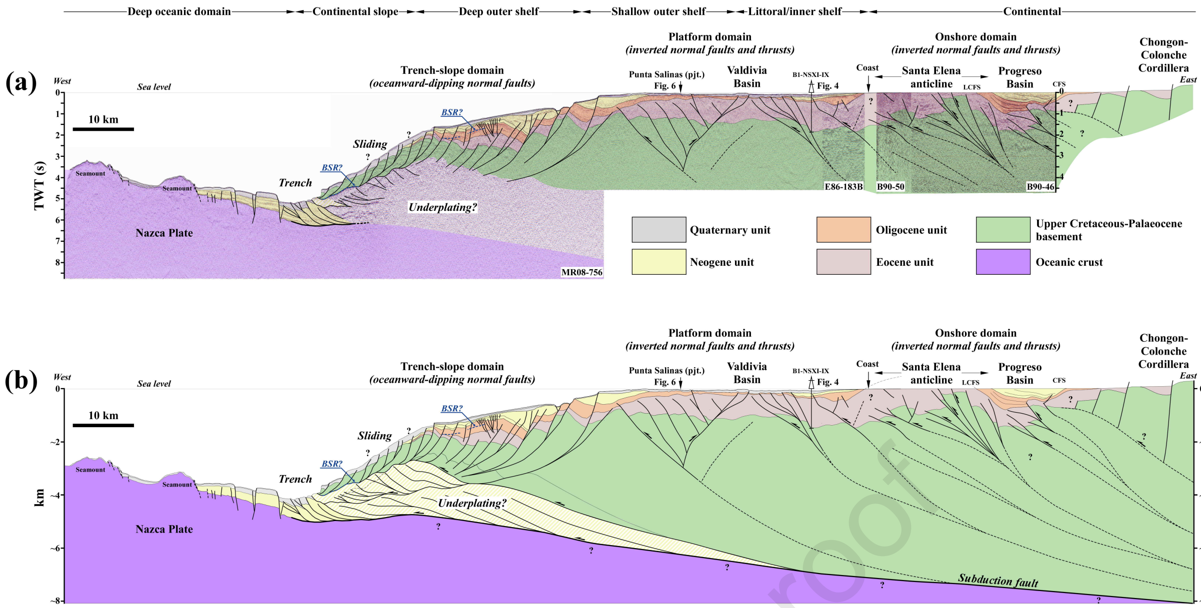
Deep oceanic domain
Continental slope
Deep outer shelf
Shallow outer shelf
Littoral/inner shelf
Continental
(a)
Platform domain
(inverted normal faults and thrusts)
Onshore domain
(inverted normal faults and thrusts)
Trench-slope domain
(oceanward-dipping normal faults)
Chongon-Colonche Cordillera
West
East
Sea level
Punta Salinas (pjt.) Fig. 6
Valdivia Basin
Coast
Santa Elena anticline
Progreso Basin
LCFS
CFS
10 km
TWT (s)
Sliding
Trench
BSR?
Underplating?
Nazca Plate
Seamount
MR08-756
E86-183B
B90-50
B90-46
Quaternary unit
Oligocene unit
Upper Cretaceous-Palaeocene basement
Neogene unit
Eocene unit
Oceanic crust
(b)
km
Subduction fault

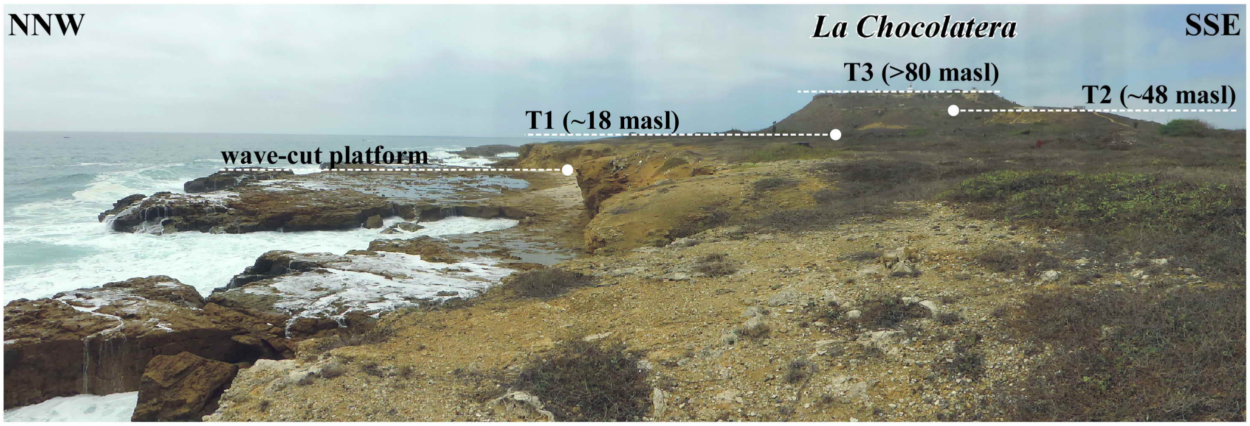
NNW
La Chocolatera
SSE
T3 (>80 masl)
T2 (~48 masl)
T1 (~18 masl)
wave-cut platform

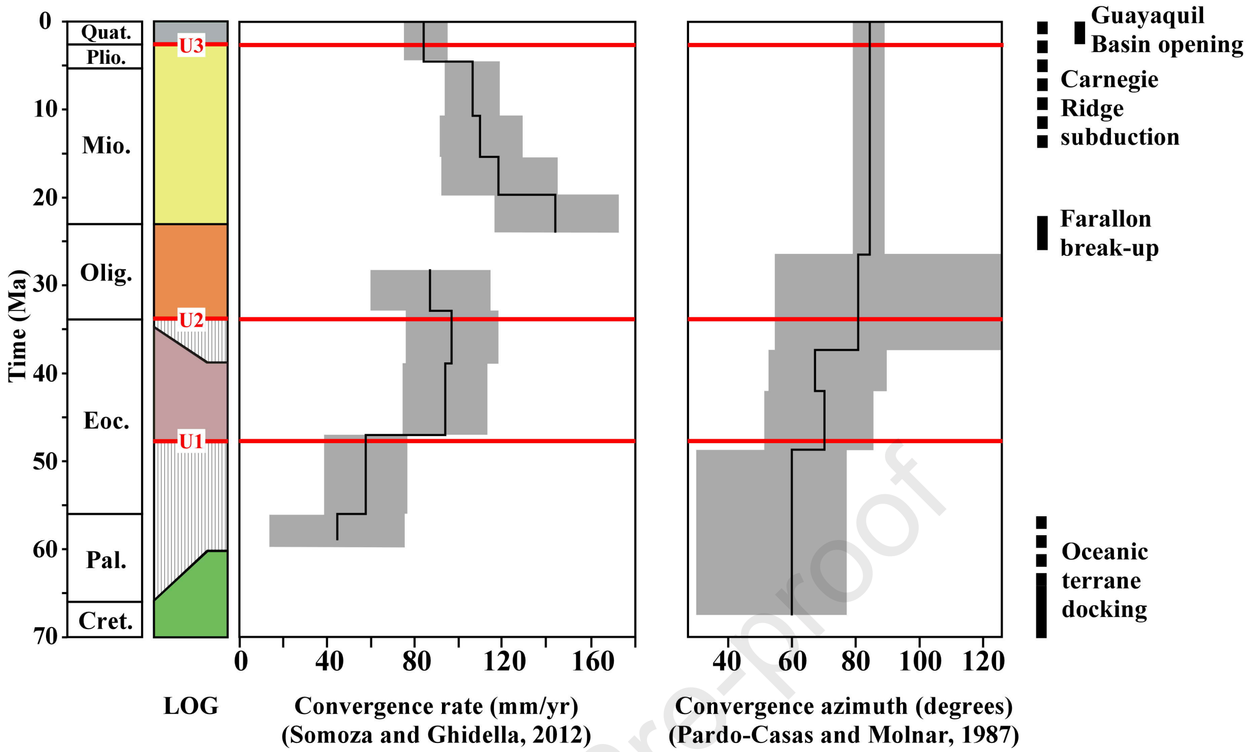
Time (Ma)
0
10
20
30
40
50
60
70
Quat.
Plio.
Mio.
Olig.
Eoc.
Pal.
Cret.
U3
U2
U1
LOG
0
40
80
120
160
Convergence rate (mm/yr)
(Somoza and Ghidella, 2012)
40
60
80
100
120
Convergence azimuth (degrees)
(Pardo-Casas and Molnar, 1987)
Guayaquil
Basin opening
Carnegie
Ridge
subduction
Farallon
break-up
Oceanic
terrane
docking

Declaration of interests

☐ The authors declare that they have no known competing financial interests or personal relationships that could have appeared to influence the work reported in this paper.

☒ The authors declare the following financial interests/personal relationships which may be considered as potential competing interests:

Cedric Bulois reports financial support was provided by French Research Institute for sustainable development (IRD). Marianne Saillard reports financial support was provided by French National Research Agency. Cédric Bulois and co-authors declare that there is no conflict of interest regarding the proposed data to illustrate the manuscript entitled "Structural evolution of the southern Ecuadorian forearc in the Santa Elena Peninsula region". This study is part of the ANR-MARACAS (ANR-18-CE31-0022). Funding agencies of this study are acknowledged in the present manuscript. Data suppliers are also acknowledged and part of the authorship of the manuscript.